Published for SISSA by Springer

Received: May 15, 2018
Revised: August 28, 2018
Accepted: October 27, 2018
Published: November 7, 2018

Search for black holes and sphalerons in high-multiplicity final states in proton-proton collisions at $\sqrt{s} = 13$ TeV

The CMS collaboration

E-mail: cms-publication-committee-chair@cern.ch

Abstract: A search in energetic, high-multiplicity final states for evidence of physics beyond the standard model, such as black holes, string balls, and electroweak sphalerons, is presented. The data sample corresponds to an integrated luminosity of 35.9 fb^{-1} collected with the CMS experiment at the LHC in proton-proton collisions at a center-of-mass energy of 13 TeV in 2016. Standard model backgrounds, dominated by multijet production, are determined from control regions in data without any reliance on simulation. No evidence for excesses above the predicted background is observed. Model-independent 95% confidence level upper limits on the cross section of beyond the standard model signals in these final states are set and further interpreted in terms of limits on semiclassical black hole, string ball, and sphaleron production. In the context of models with large extra dimensions, semiclassical black holes with minimum masses as high as 10.1 TeV and string balls with masses as high as 9.5 TeV are excluded by this search. Results of the first dedicated search for electroweak sphalerons are presented. An upper limit of 0.021 is set at 95% confidence level on the fraction of all quark-quark interactions above the nominal threshold energy of 9 TeV resulting in the sphaleron transition.

Keywords: Beyond Standard Model, Hadron-Hadron scattering (experiments)

ArXiv ePrint: 1805.06013

We dedicate this paper to the memory of Prof. Stephen William Hawking, on whose transformative ideas much of this work relies.

https://doi.org/10.1007/JHEP11(2018)042

JHEP11(2018)042

Contents

JHEP11(2018)042

1 Introduction

Many theoretical models of physics beyond the standard model (SM) [1–3] predict strong production of particles decaying into high-multiplicity final states, i.e., characterized by three or more energetic jets, leptons, or photons. Among these models are supersymmetry [4–11], with or without R-parity violation [12], and models with low-scale quantum gravity [13–17], strong dynamics, or other nonperturbative physics phenomena. While the final states predicted in these models differ significantly in the type of particles produced, their multiplicity, and the transverse momentum imbalance, they share the common feature

of a large number of energetic objects (jets, leptons, and/or photons) in the final state. The search described in this paper targets these models of beyond-the-SM (BSM) physics by looking for final states of various inclusive multiplicities featuring energetic objects. Furthermore, since such final states can be used to test a large variety of models, we provide model-independent exclusions on hypothetical signal cross sections. Considering concrete examples of such models, we interpret the results of the search explicitly in models with microscopic semiclassical black holes (BHs) and string balls (SBs), as well as in models with electroweak (EW) sphalerons. These examples are discussed in detail in the rest of this section.

1.1 Microscopic black holes

In our universe, gravity is the weakest of all known forces. Indeed, the Newton constant, $\sim 10^{-38}\,\mathrm{GeV}^{-2}$, which governs the strength of gravity, is much smaller than the Fermi constant, $\sim 10^{-4}\,\mathrm{GeV}^{-2}$, which characterizes the strength of EW interactions. Consequently, the Planck scale $M_{\mathrm{Pl}} \sim 10^{19}\,\mathrm{GeV}$, i.e., the energy at which gravity is expected to become strong, is 17 orders of magnitude higher than the EW scale of $\sim$100 GeV. With the discovery of the Higgs boson [18–20] with a mass [21, 22] at the EW scale, the large difference between the two scales poses what is known as the hierarchy problem [23]. This is because in the SM, the Higgs boson mass is not protected against quadratically divergent quantum corrections and — in the absence of fine tuning — is expected to be naturally at the largest energy scale of the theory: the Planck scale. A number of theoretical models have been proposed that attempt to solve the hierarchy problem, such as supersymmetry, technicolor [24], and, more recently, theoretical frameworks based on extra dimensions in space: the Arkani-Hamed, Dimopoulos, and Dvali (ADD) model [13–15] and the Randall–Sundrum model [16, 17].

In this paper, we look for the manifestation of the ADD model that postulates the existence of $n_{\mathrm{ED}} \geq 2$ "large" (compared to the inverse of the EW energy scale) extra spatial dimensions, compactified on a sphere or a torus, in which only gravity can propagate. This framework allows one to elude the hierarchy problem by explaining the apparent weakness of gravity in the three-dimensional space via the suppression of the fundamentally strong gravitational interaction by the large volume of the extra space. As a result, the fundamental Planck scale, M_{D}, in $3 + n_{\mathrm{ED}}$ dimensions is related to the apparent Planck scale in 3 dimensions via Gauss's law as: ${M_{\mathrm{Pl}}}^2 \sim {M_{\mathrm{D}}}^{n_{\mathrm{ED}}+2} R^{n_{\mathrm{ED}}}$, where R is the radius of extra dimensions. Since M_{D} could be as low as a few TeV, i.e., relatively close to the EW scale, the hierarchy problem would be alleviated.

At high-energy colliders, one of the possible manifestations of the ADD model is the formation of microscopic BHs [25, 26] with a production cross section proportional to the squared Schwarzschild radius, given as:

$$R_{\mathrm{S}} = \frac{1}{\sqrt{\pi} M_{\mathrm{D}}} \left[\frac{M_{\mathrm{BH}}}{M_{\mathrm{D}}} \left(\frac{8\Gamma(\frac{n_{\mathrm{ED}}+3}{2})}{n_{\mathrm{ED}}+2} \right) \right]^{\frac{1}{n_{\mathrm{ED}}+1}},$$

where Γ is the gamma function and M_{BH} is the mass of the BH. In the simplest production scenario, the cross section is given by the area of a disk of radius R_{S}, i.e., $\sigma \approx \pi {R_{\mathrm{S}}}^2$ [25,

JHEP11(2018)042

26]. In more complicated production scenarios, e.g., a scenario with energy loss during the formation of the BH horizon, the cross section is modified from this "black disk" approximation by a factor of order one [26].

As BH production is a threshold phenomenon, we search for BHs above a certain minimum mass $M_{\mathrm{BH}}^{\mathrm{min}} \geq M_{\mathrm{D}}$. In the absence of signal, we will express the results of the search as limits on $M_{\mathrm{BH}}^{\mathrm{min}}$. In the semiclassical case (strictly valid for $M_{\mathrm{BH}} \gg M_{\mathrm{D}}$), the BH quickly evaporates via Hawking radiation [27] into a large number of energetic particles, such as gluons, quarks, leptons, photons, etc. The relative abundance of various particles produced in the process of BH evaporation is expected to follow the number of degrees of freedom per particle in the SM. Thus, about 75% of particles produced are expected to be quarks and gluons, because they come in three or eight color combinations, respectively. A significant amount of missing transverse momentum may be also produced in the process of BH evaporation via production of neutrinos, which constitute ∼5% of the products of a semiclassical BH decay, W and Z boson decays, heavy-flavor quark decays, gravitons, or noninteracting stable BH remnants.

If the mass of a BH is close to M_{D}, it is expected to exhibit quantum features, which can modify the characteristics of its decay products. For example, quantum BHs [28–30] are expected to decay before they thermalize, resulting in low-multiplicity final states. Another model of semiclassical BH precursors is the SB model [31], which predicts the formation of a long, jagged string excitation, folded into a "ball". The evaporation of an SB is similar to that of a semiclassical BH, except that it takes place at a fixed Hagedorn temperature [32], which depends only on the string scale M_{S}. The formation of an SB occurs once the mass of the object exceeds $M_{\mathrm{S}}/g_{\mathrm{S}}$, where g_{S} is the string coupling. As the mass of the SB grows, eventually it will transform into a semiclassical BH, once its mass exceeds $M_{\mathrm{S}}/{g_{\mathrm{S}}}^2 > M_{\mathrm{D}}$.

A number of searches for both semiclassical and quantum BHs, as well as for SBs have been performed at the CERN LHC using the Run 1 ($\sqrt{s} = 7$ and 8 TeV) and Run 2 ($\sqrt{s} =$ 13 TeV) data. An extensive review of Run 1 searches can be found in ref. [33]. The most recent Run 2 searches for semiclassical BHs and SBs were carried out by ATLAS [34, 35] and CMS [36] using 2015 data. Results of searches for quantum BHs in Run 2 based on 2015 and 2016 data can be found in refs. [37–42]. The most stringent limits on $M_{\mathrm{BH}}^{\mathrm{min}}$ set by the Run 2 searches are 9.5 and 9.0 TeV for semiclassical and quantum BHs, respectively, for $M_{\mathrm{D}} = 4$ TeV [34, 36]. The analogous limits on the minimum SB mass depend on the choice of the string scale and coupling and are in the 6.6 − 9 TeV range for the parameter choices considered in refs. [34, 36].

1.2 Sphalerons

The Lagrangian of the EW sector of the SM has a possible nonperturbative solution, which includes a vacuum transition known as a "sphaleron". This class of solutions to gauge field theories was first proposed in 1976 by 't Hooft [43]. The particular sphaleron solution of the SM was first described by Klinkhamer and Manton in 1984 [44]. It is also a critical piece of EW baryogenesis theory [45], which explains the matter-antimatter asymmetry of the universe by such processes. The crucial feature of the sphaleron, which allows such claims to be made, is the violation of baryon (B) and lepton (L) numbers, while preserving $B - L$.

JHEP11(2018)042

The possibility of sphaleron transitions at hadron colliders and related phenomenology has been discussed since the late 1980s [46].

Within the framework of perturbative SM physics, there are twelve globally conserved currents, one for each of the 12 fundamental fermions: $J^\mu = \overline{\psi}_L \gamma^\mu \psi_L$. An anomaly breaks this conservation, in particular $\partial_\mu J^\mu = [g^2/(16\pi^2)]\mathrm{Tr}[F_{\mu\nu}\widetilde{F}^{\mu\nu}]$. This is because the integral of this term, known as a Chern–Simons (or winding) number N_{CS} [47], is nonzero. The anomaly exists for each fermion doublet. This means that the lepton number changes by $3N_{\mathrm{CS}}$, since each of three leptons produced has absolute lepton number of 1. The baryon number will also change by $3N_{\mathrm{CS}}$ because each quark has an absolute baryon number of 1/3 and there are three colors and three generations of quarks produced. This results in two important relations, which are essential to the phenomenology of sphalerons: $\Delta(B+L) = 6N_{\mathrm{CS}}$ and $\Delta(B-L) = 0$. The anomaly only exists if there is enough energy to overcome the potential in N_{CS}, which is fixed by the values of the EW couplings. Assuming the state at 125 GeV to be the SM Higgs boson, the precise measurement of its mass [21, 22] allowed the determination of these couplings, giving an estimate of the energy required for the sphaleron transitions of $E_{\mathrm{sph}} \approx 9\,\mathrm{TeV}$ [44, 48].

While the E_{sph} threshold is within the reach of the LHC, it was originally thought that the sphaleron transition probability would be significantly suppressed by a large potential barrier. However, in a recent work [48] it has been suggested that the periodic nature of the Chern–Simons potential reduces this suppression at collision energies $\sqrt{\hat{s}} < E_{\mathrm{sph}}$, removing it completely for $\sqrt{\hat{s}} \geq E_{\mathrm{sph}}$. This argument opens up the possibility of observing an EW sphaleron transition in proton-proton (pp) collisions at the LHC via processes such as: $\mathrm{u} + \mathrm{u} \to \mathrm{e}^+\mu^+\tau^+\,\overline{\mathrm{t}}\,\overline{\mathrm{t}}\,\overline{\mathrm{b}}\,\overline{\mathrm{c}}\,\overline{\mathrm{c}}\,\overline{\mathrm{s}}\,\overline{\mathrm{d}} + X$. Fundamentally, the $N_{\mathrm{CS}} = +1$ (-1) sphaleron transitions involve 12 (anti)fermions: three (anti)leptons, one from each generation, and nine (anti)quarks, corresponding to three colors and three generations, with the total electric charge and weak isospin of zero. Nevertheless, at the LHC, we consider signatures with 14, 12, or 10 particles produced, that arise from a $\mathrm{q} + \mathrm{q}' \to \mathrm{q} + \mathrm{q}' +$ sphaleron process, where 0, 1, or 2 of the 12 fermions corresponding to the sphaleron transition may "cancel" the q or q′ inherited from the initial state [49, 50]. Since between zero and three of the produced particles are neutrinos, and also between zero and three are top quarks, which further decay, the actual multiplicity of the visible final-state particles may vary between 7 and 20 or more. Some of the final-state particles may also be gluons from either initial- or final-state radiation. While the large number of allowed combinations of the 12 (anti)fermions results in over a million unique transitions [51], many of the final states resulting from these transitions would look identical in a typical collider experiment, as no distinction is made between quarks of the first two generations, leading to only a few dozen phenomenologically unique transitions, determined by the charges and types of leptons and the third-generation quarks in the final state. These transitions would lead to characteristic collider signatures, which would have many energetic jets and charged leptons, as well as large missing transverse momentum due to undetected neutrinos.

A phenomenological reinterpretation in terms of limits on the EW sphaleron production of an ATLAS search for microscopic BHs in the multijet final states at $\sqrt{s} = 13\,\mathrm{TeV}$ [34], comparable to an earlier CMS analysis [36], was recently performed in ref. [49]. In the present paper, we describe the first dedicated experimental search for EW sphaleron transitions.

JHEP11(2018)042

2 The CMS detector and the data sample

The central feature of the CMS apparatus is a superconducting solenoid of 6 m internal diameter, providing a magnetic field of 3.8 T. Within the solenoid volume are a silicon pixel and strip tracker, a lead tungstate crystal electromagnetic calorimeter (ECAL), and a brass and scintillator hadron calorimeter (HCAL), each composed of a barrel and two endcap sections. Forward calorimeters extend the pseudorapidity (η) coverage provided by the barrel and endcap detectors. Muons are detected in gas-ionization chambers embedded in the steel flux-return yoke outside the solenoid.

In the region $|\eta| < 1.74$, the HCAL cells have widths of 0.087 in pseudorapidity and 0.087 in azimuth (ϕ). In the $\eta - \phi$ plane, and for $|\eta| < 1.48$, the HCAL cells map on to 5×5 arrays of ECAL crystals to form calorimeter towers projecting radially outwards from close to the nominal interaction point. For $|\eta| > 1.74$, the coverage of the towers increases progressively to a maximum of 0.174 in $\Delta\eta$ and $\Delta\phi$. Within each tower, the energy deposits in ECAL and HCAL cells are summed to define the calorimeter tower energies, subsequently used to provide the energies and directions of hadronic jets.

Events of interest are selected using a two-tiered trigger system [52]. The first level, composed of custom hardware processors, uses information from the calorimeters and muon detectors to select events at a rate of around 100 kHz within a time interval of less than 4 μs. The second level, known as the high-level trigger (HLT), consists of a farm of processors running a version of the full event reconstruction software optimized for fast processing, and reduces the event rate to around 1 kHz before data storage.

A more detailed description of the CMS detector, together with a definition of the coordinate system used and the relevant kinematic variables, can be found in ref. [53].

The analysis is based on a data sample recorded with the CMS detector in pp collisions at a center-of-mass energy of 13 TeV in 2016, corresponding to an integrated luminosity of 35.9 fb^{-1}. Since typical signal events are expected to contain multiple jets, we employ a trigger based on the H_{T} variable, defined as the scalar sum of the transverse momenta (p_{T}) of all jets in an event reconstructed at the HLT. We require $H_{\mathrm{T}} > 800$–900 GeV and also use a logical OR with several single-jet triggers with p_{T} thresholds of 450–500 GeV. The resulting trigger selection is fully efficient for events that subsequently satisfy the offline requirements used in the analysis.

3 Event reconstruction

The particle-flow (PF) algorithm [54] aims to reconstruct and identify each individual particle in an event with an optimized combination of information from the various elements of the CMS detector. The energy of photons is directly obtained from the ECAL measurement, corrected for zero-suppression effects. The energy of electrons is determined from a combination of the electron momentum at the primary interaction vertex as determined by the tracker, the energy of the corresponding ECAL cluster, and the energy sum of all bremsstrahlung photons spatially compatible with originating from the electron track. The energy of muons is obtained from the curvature of the corresponding track. The energy

JHEP11(2018)042

of charged hadrons is determined from a combination of their momentum measured in the tracker and the matching ECAL and HCAL energy deposits, corrected for zero-suppression effects and for the response function of the calorimeters to hadronic showers. Finally, the energy of neutral hadrons is obtained from the corresponding corrected ECAL and HCAL energies.

The reconstructed vertex with the largest value of summed physics-object p_{T}^2 is taken to be the primary pp interaction vertex. The physics objects are the jets, clustered using the anti-k_{T} jet finding algorithm [55, 56] with the tracks assigned to the vertex as inputs, and the associated missing transverse momentum, taken as the negative vector sum of the p_{T} of those jets. Events are required to have at least one reconstructed vertex within 24 (2) cm of the nominal collision point in the direction parallel (perpendicular) to the beams.

For each event, hadronic jets are clustered from the PF candidates using the anti-k_{T} algorithm with a distance parameter of 0.4. The jet momentum is determined as the vectorial sum of all particle momenta in the jet, and is found from simulation to be within 5 to 10% of the true momentum over the whole p_{T} spectrum and detector acceptance. Additional pp interactions within the same or neighboring bunch crossings (pileup) can contribute additional tracks and calorimetric energy depositions to the jet momentum. To mitigate this effect, tracks originating from pileup vertices are discarded and an offset correction is applied to correct for the remaining contributions. Jet energy corrections are derived from simulation, to bring the measured response of jets to that of particle-level jets on average. In situ measurements of the momentum balance in dijet, multijet, γ+jet, and leptonically decaying Z+jet events are used to account for any residual differences in the jet energy scales in data and simulation [57]. The jet energy resolution amounts typically to 15% at a jet p_{T} of 10 GeV, 8% at 100 GeV, and 4% at 1 TeV. Additional selection criteria are applied to each jet to remove those potentially dominated by anomalous contributions from various subdetector components or reconstruction failures. All jets are required to have $p_{\mathrm{T}} > 70$ GeV and be within $|\eta| < 5$. For the leading p_{T} jet in each event, the energy fraction carried by muon candidates failing the standard identification [58] is required to be less than 80%. This requirement removes events where a low-momentum muon is misreconstructed with very high momentum and misidentified as a high-energy jet. We further require the leading jet in an event to have a charged-hadron fraction of less than 0.99 if this jet is found within $|\eta| < 2.4$ [59].

The missing transverse momentum, $p_{\mathrm{T}}^{\mathrm{miss}}$, is defined as the magnitude of the vectorial sum of transverse momenta of all PF candidates in an event. The jet energy corrections are further propagated to the $p_{\mathrm{T}}^{\mathrm{miss}}$ calculation.

Details of muon reconstruction can be found in ref. [58]. The muon candidate is required to have at least one matching energy deposit in the pixel tracker and at least six deposits in the silicon strip tracker, as well as at least two track segments in the muon detector. The transverse impact parameter and the longitudinal distance of the track associated with the muon with respect to the primary vertex are required to be less than 2 and 5 mm, respectively, to reduce contamination from cosmic ray muons. The global track fit to the tracker trajectory and to the muon detector segments must have a χ^2 per degree of freedom of less than 10. Muon candidates are required to have $p_{\mathrm{T}} > 70$ GeV and to be within $|\eta| < 2.4$.

JHEP11(2018)042

Details of electron and photon reconstruction can be found in refs. [60] and [61], respectively. Electron and photon candidates are required to have $p_T > 70$ GeV and $|\eta| < 2.5$, excluding the $1.44 < |\eta| < 1.57$ transition region between the ECAL barrel and endcap detectors where the reconstruction is suboptimal. We use standard identification criteria, corresponding to an average efficiency of 80% per electron or photon. The identification criteria include a requirement that the transverse size of the electromagnetic cluster be compatible with the one expected from a genuine electron or photon, and that the ratio of the HCAL to ECAL energies be less then 0.25 (0.09) for electrons and less than 0.0396 (0.0219) for photons in the barrel (endcap). In addition, photon candidates are required to pass the conversion-safe electron veto requirements [61], which disambiguates them from electron candidates.

Muons, electrons, and photons are required to be isolated from other energy deposits in the tracker and the calorimeters. The isolation $\mathcal{I}$ is defined as the ratio of the p_T sum of various types of additional PF candidates in a cone of radius $\Delta R = \sqrt{(\Delta\eta)^2 + (\Delta\phi)^2}$ of 0.4 (muons) or 0.3 (electrons and photons), centered on the lepton or photon candidate, to the candidate's p_T. For muons, the numerator of the ratio is corrected for the contribution of neutral particles due to pileup, using one half of the p_T carried by the charged hadrons originating from pileup vertices. For electrons and photons, an average area method [62], as estimated with FastJet [56], is used. The isolation requirements are the same as used in an earlier 13 TeV analysis [36], except that for electrons we use a tighter isolation requirement of $\mathcal{I} < 0.07$.

To avoid double counting, we remove jets that are found within a radius of $\Delta R = 0.3$ from a muon, electron, or photon, if the latter object contributes more than 80, 70, or 50% of the jet p_T, respectively.

4 Analysis strategy

We follow closely the approach for semiclassical BH searches originally developed by CMS for Run 1 analyses [63–65] and subsequently used in the studies of early Run 2 [36] data. This approach is based on an inclusive search for BH decays to all possible final states, dominated by the high-multiplicity multijet ones in the semiclassical BH case. This type of analysis is less sensitive to the details of BH evaporation and the relative abundance of various particles produced, as it considers all types of particles in the final state. We use a single discriminating variable S_T, defined as the scalar sum of p_T of all N energetic objects in an event (which we define as jets, electrons, muons, and photons with p_T above a given threshold), plus p_T^{miss} in the event, if it exceeds the same threshold: $S_T = p_T^{miss} + \sum_{i=1}^{N} p_T^i$. Accounting for p_T^{miss} in the S_T variable makes S_T a better measure of the total transverse momentum in the event carried by all the various particles. Since it is impossible to tell how many objects lead to the p_T^{miss} in the event, we do not consider p_T^{miss} values above the threshold when determining the object multiplicity.

This definition of S_T is robust against variations in the BH evaporation model, and is also sensitive to the cases when there is large p_T^{miss} due to enhanced emission of gravitons or to models in which a massive, weakly interacting remnant of a BH is formed at the

JHEP11(2018)042

terminal stage of Hawking evaporation, with a mass below M_D. It is equally applicable to sphaleron searches, given the expected energetic, high-multiplicity final states, possibly with large p_T^{miss}.

The S_T distributions are then considered separately for various inclusive object multiplicities (i.e., $N \geq N^{min} = 3, \ldots, 11$). The background is dominated by SM QCD multijet production and is estimated exclusively from control samples in data. The observed number of events with S_T values above a chosen threshold is compared with the background and signal+background predictions to either establish a signal or to set limits on the signal production. This approach does not rely on the Monte Carlo (MC) simulation of the backgrounds, and it also has higher sensitivity than exclusive searches in specific final states, e.g., lepton+jets [66, 67].

The main challenge of the search is to describe the inclusive multijet background in a robust way, as both BH and sphaleron signals correspond to a broad enhancement in the high tail of the S_T distribution, rather than to a narrow peak. Since these signals are expected to involve a high multiplicity of final-state particles, one has to reliably describe the background for large jet multiplicities, which is quite challenging theoretically as higher-order calculations that fully describe multijet production do not exist. Thus, one cannot rely on simulation to reproduce the S_T spectrum for large N correctly.

To overcome this problem, a dedicated method of predicting the QCD multijet background directly from collision data has been developed for the original Run 1 analysis [63] and used in the subsequent Run 1 [64, 65] and Run 2 [36] searches. It has been found empirically, first via simulation-based studies, and then from the analysis of data at low jet multiplicities, that the shape of the S_T distribution for the dominant QCD multijet background does not depend on the multiplicity of the final state, above a certain turn-on threshold. This observation reflects the way a parton shower develops via nearly collinear emission, which conserves S_T. It allows one to predict the S_T spectrum of a multijet final state using low-multiplicity QCD events, e.g., dijet or trijet events. This "S_T invariance" provides a powerful method of predicting the dominant background for BH production by taking the S_T shape from low-multiplicity events, for which the signal contamination is expected to be negligible, and normalizing it to the observed spectrum at high multiplicities at the low end of the S_T distribution, where signal contamination is negligible even for large multiplicities of the final-state objects. The method has been also used for other CMS searches, e.g., a search for stealth supersymmetry [68] and a search for multijet resonances [69].

5 Simulated samples

5.1 Black hole and string ball signal samples

Signal simulation is performed using the BlackMax v2.02.0 [70] (semiclassical BHs) and charybdis 2 v1.003 [71, 72] (semiclassical BHs and SBs) generators. The generator settings of each model are listed in tables 1 and 2.

For semiclassical BH signals, we explore different aspects of BH production and decay by simulating various scenarios, including nonrotating BHs (B1,C2), rotating BHs (B2,C1), rotating BHs with mass loss (B3), and rotating BHs with Yoshino–Rychkov bounds [73]

JHEP11(2018)042

Model	Choose_a_case	Mass_loss_factor	Momentum_loss_factor	turn_on_graviton
B1	tensionless_nonrotating	0	0	FALSE
B2	rotating_nonsplit	0	0	FALSE
B3	rotating_nonsplit	0.1	0.1	TRUE

Table 1. Generator settings used for BlackMax signal sample generation.

Model	BHSPIN	MJLOST	YRCSC	NBODYAVERAGE	NBODYPHASE	NBODYVAR	RMSTAB	RMBOIL
C1	TRUE	FALSE	FALSE	FALSE	TRUE	TRUE	FALSE	FALSE
C2	FALSE	FALSE	FALSE	FALSE	TRUE	TRUE	FALSE	FALSE
C3	TRUE	FALSE	FALSE	TRUE	FALSE	FALSE	FALSE	FALSE
C4	TRUE	TRUE	TRUE	FALSE	TRUE	TRUE	FALSE	FALSE
C5	TRUE	TRUE	TRUE	FALSE	FALSE	FALSE	TRUE	FALSE
C6	TRUE	TRUE	TRUE	FALSE	FALSE	FALSE	FALSE	TRUE

Table 2. Generator settings used for CHARYBDIS 2 signal sample generation.

(C4). Models C3, C5, and C6 explore the termination phase of the BH with different object multiplicities from the BH remnant, varying from 2-body decaying remnant (C3), stable remnant (C5, for which additionally the generator parameter NBODY was changed from its default value of 2 to 0), and "boiling" remnant (C6), where the remnant continues to evaporate until a maximum Hawking temperature equal to M_{D} is reached. For each model, the fundamental Planck scale M_{D} is varied within 2–9 TeV in 1 TeV steps, each with $n_{\mathrm{ED}} = 2, 4, 6$. The minimum black hole mass $M_{\mathrm{BH}}^{\mathrm{min}}$ is varied between $M_{\mathrm{D}} + 1$ TeV and 11 TeV in 1 TeV steps.

For SB signals, two sets of benchmark points are generated with CHARYBDIS 2, such that different regimes of the SB production can be explored. For a constant string coupling value $g_{\mathrm{S}} = 0.2$ the string scale M_{S} is varied from 2 to 4 TeV, while at constant $M_{\mathrm{S}} = 3.6$ TeV, g_{S} is varied from 0.2 to 0.4. For all SB samples, $n_{\mathrm{ED}} = 6$ is used. The SB dynamics below the first transition ($M_{\mathrm{S}}/g_{\mathrm{S}}$), where the SB production cross section scales with ${g_{\mathrm{S}}}^2/{M_{\mathrm{S}}}^4$, are probed with the constant $g_{\mathrm{S}} = 0.2$ and low M_{S} values as well as with the constant M_{S} scan. The saturation regime ($M_{\mathrm{S}}/g_{\mathrm{S}} < M_{\mathrm{SB}} < M_{\mathrm{S}}/{g_{\mathrm{S}}}^2$), where the SB production cross section no longer depends on g_{S}, is probed by the higher M_{S} points of the constant g_{S} benchmark. For each benchmark point, the scale M_{D} is chosen such that the cross section at the SB-BH transition ($M_{\mathrm{S}}/{g_{\mathrm{S}}}^2$) is continuous.

For the BH and SB signal samples we use leading order (LO) MSTW2008LO [74, 75] parton distribution functions (PDFs). This choice is driven by the fact that this set tends to give a conservative estimate of the signal cross section at high masses, as checked with the modern NNPDF3.0 [76] LO PDFs, with the value of strong coupling constant of 0.118 used for the central prediction, with a standard uncertainty eigenset. The MSTW2008LO PDF set was also used in all Run 1 BH searches [63–65] and in an earlier Run 2 [36] search, which makes the comparison with earlier results straightforward.

JHEP11(2018)042

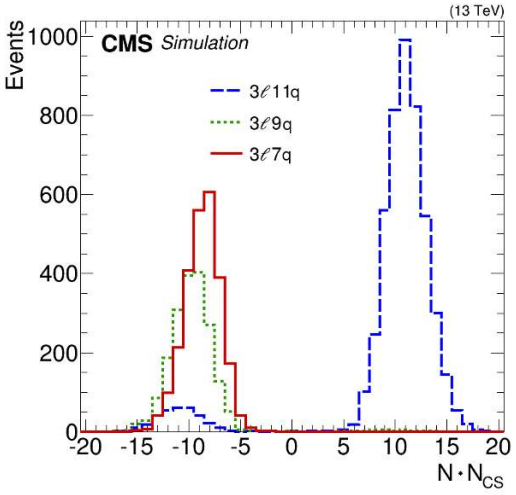

Figure 1. Observed final-state particle multiplicity N distributions for $N_{CS} = \pm 1$ sphaleron transitions resulting in 10, 12, and 14 parton-level final-state multiplicities. The relative numbers of events in the histograms are proportional to the relative probabilities of these three parton-level configurations. The peaks at positive values correspond to $N_{CS} = 1$ transitions, while those at negative values correspond to $N_{CS} = -1$ transitions and therefore are shifted toward lower multiplicity N because of cancellations with initial-state partons.

5.2 Sphaleron signal samples

The electroweak sphaleron processes are generated at LO with the BaryoGEN v1.0 generator [50], capable of simulating various final states described in section 1.2. We simulate the sphaleron signal for three values of the transition energy $E_{sph} = 8$, 9, and 10 TeV. The parton-level simulation is done with the CT10 LO PDF set [77]. In the process of studying various PDF sets, we found that the NNPDF3.0 yields a significantly larger fraction of sea quarks in the kinematic region of interest than all other modern PDFs. While the uncertainty in this fraction is close to 100%, we chose the CT10 set, for which this fraction is close to the median of the various PDF sets we studied. The PDF uncertainties discussed in section 7 cover the variation in the signal acceptance between various PDFs due to this effect.

The typical final-state multiplicities for the $N_{CS} = \pm 1$ sphaleron transitions resulting in 10, 12, or 14 parton-level final states are shown in figure 1. The $N_{CS} = 1$ transitions are dominated by 14 final-state partons, as the proton mainly consists of valence quarks, thus making the probability of cancellations small.

The cross section for sphaleron production is given by [49]: $\sigma = \mathrm{PEF}\,\sigma_0$, where $\sigma_0 = 121$, 10.1, and 0.51 fb for $E_{sph} = 8$, 9, and 10 TeV, respectively, and PEF is the pre-exponential factor, defined as the fraction of all quark-quark interactions above the sphaleron energy threshold E_{sph} that undergo the sphaleron transition.

5.3 Background samples

In addition, we use simulated samples of W+jets, Z+jets, γ+jets, $t\bar{t}$, and QCD multijet events for auxiliary studies. These events are generated with the MadGraph5_aMC@NLO

JHEP11(2018)042

v2.2.2 [78] event generator at LO or next-to-LO, with the NNPDF3.0 PDF set of a matching order.

The fragmentation and hadronization of parton-level signal and background samples is done with PYTHIA v8.205 [79], using the underlying event tune CUETP8M1 [80]. All signal and background samples are reconstructed with the detailed simulation of the CMS detector via GEANT4 [81]. The effect of pileup interactions is simulated by superimposing simulated minimum bias events on the hard-scattering interaction, with the multiplicity distribution chosen to match the one observed in data.

6 Background estimate

6.1 Background composition

The main backgrounds in the analyzed multi-object final states are: QCD multijet, V+jets (where V = W, Z), γ+jets, and $\mathrm{t\bar{t}}$ production, with the QCD multijet background being by far the most dominant. Figure 2 illustrates the relative importance of these backgrounds for the inclusive multiplicity $N \geq 3$ and 6 cases, based on simulated background samples. To reach the overall agreement with the data, all simulated backgrounds except for the QCD multijets are normalized to the most accurate theoretical predictions available, while the QCD multijet background is normalized so that the total number of background events matches that in data. While we do not use simulated backgrounds to obtain the main results in this analysis, figure 2 illustrates an important point: not only is the QCD multijet background at least an order of magnitude more important than other backgrounds, for both low- and high-multiplicity cases, but also the shape of the S_T distributions for all major backgrounds is very similar, so the method we use to estimate the multijet background, discussed below, provides an acceptable means of predicting the overall background as well.

6.2 Background shape determination

The background prediction method used in the analysis follows closely that in previous similar CMS searches [36, 63–65]. As discussed in section 4, the central idea of this method is that the shape of the S_T distribution for the dominant multijet background is invariant with respect to the final-state object multiplicity N. Consequently, the background shape can be extracted from low-multiplicity spectra and used to describe the background at high multiplicities. The S_T value is preserved by the final-state radiation, which is the dominant source of extra jets beyond LO $2 \to 2$ QCD processes, as long as the additional jets are above the p_T threshold used in the definition of S_T. At the same time, jets from initial-state radiation (ISR) change the S_T value, but because their p_T spectrum is steeply falling they typically contribute only a few percent to the S_T value and change the multiplicity N by just one unit, for events used in the analysis. Consequently, we extract the background shape from the $N = 3$ S_T spectrum, which already has a contribution from ISR jets, and therefore reproduces the S_T shape at higher multiplicities better than the $N = 2$ spectrum used in earlier analyses. To estimate any residual noninvariance in the S_T distribution, the $N = 4$ S_T spectrum, normalized to the $N = 3$ spectrum in terms of the total number

JHEP11(2018)042

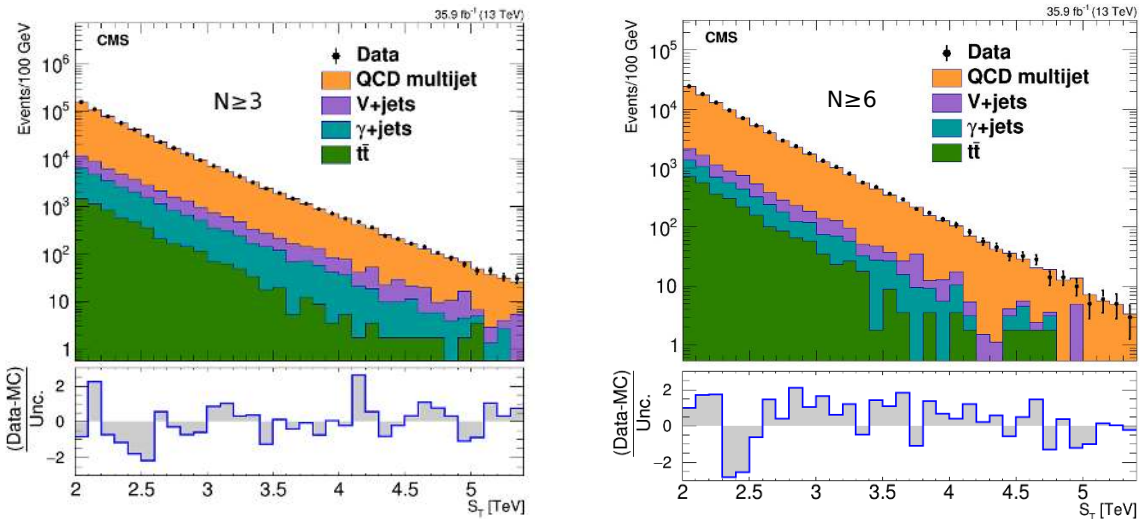

Figure 2. The S_{T} distribution in data for inclusive multiplicities of (left) $N \geq 3$ and (right) $N \geq 6$, compared with the normalized background prediction from simulation, illustrating the relative contributions of major backgrounds. The lower panels show the difference between the data and the simulated background prediction, divided by the statistical uncertainty in data. We note that despite an overall agreement, we do not rely on simulation for obtaining the background prediction.

of events, is also used as an additional component of the background shape uncertainty. Furthermore, to be less sensitive to the higher instantaneous luminosity delivered by the LHC in 2016, which resulted in a higher pileup, and to further reduce the effect of ISR, the p_{T} threshold for all objects was raised to 70 GeV, compared to 50 GeV used in earlier analyses. The reoptimization that has resulted in the choice of a new exclusive multiplicity to be used for the baseline QCD multijet background prediction and a higher minimum p_{T} threshold for the objects counted toward S_{T} was based on extensive studies of MC samples and low-S_{T} events in data.

In order to obtain the background template, we use a set of 16 functions employed in earlier searches for BSM physics in dijets, VV events, and multijet events at various colliders. These functions typically have an exponential or power-law behavior with S_{T}, and are described by 3–5 free parameters. Some of the functions are monotonously falling with S_{T} by construction; however, some of them contain polynomial terms, such that they are not constrained to have a monotonic behavior. In order to determine the background shape, we fit the $N = 3$ S_{T} distribution or the $N = 4$ S_{T} distribution, normalized to the same total event count as the $N = 3$ distribution, in the range of 2.5–4.3 TeV, where any sizable contributions from BSM physics have been ruled out by earlier versions of this analysis, with all 16 functional forms. The lowest masses of the signal models considered, which have not been excluded by the previous analysis [36], contribute less than 2% to the total number of events within the fit range. Any functional form observed not to be monotonically decreasing up to $S_{\mathrm{T}} = 13$ TeV after the fit to both multiplicities is discarded. The largest spread among all the accepted functions in the $N = 3$ and $N = 4$ fits is used as an envelope of the systematic uncertainty in the background template. The use of both $N = 3$ and $N = 4$ distributions

JHEP11(2018)042

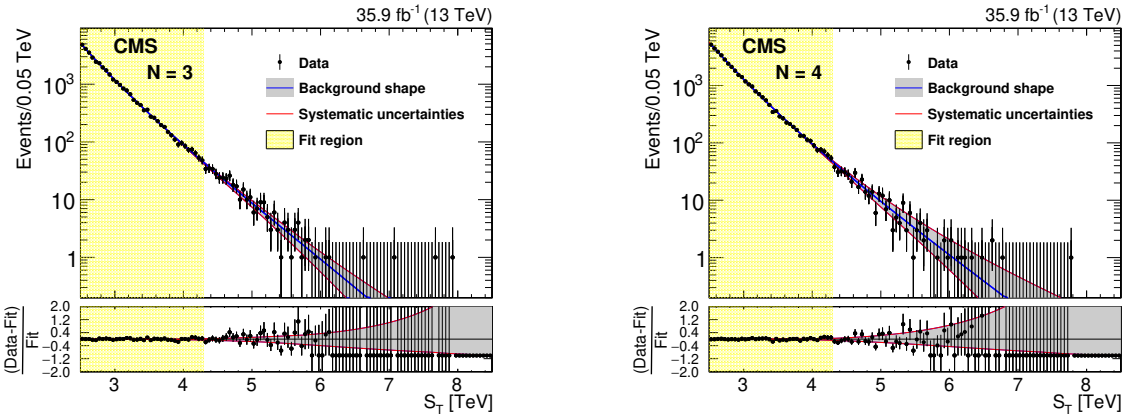

Figure 3. The results of the fit to data with $N = 3$ (left) and $N = 4$ (right), after discarding the functions that fail to monotonically decrease up to $S_T = 13\,\text{TeV}$. The description of the best fit function and the envelope are given in the main text. A few points beyond the plotted vertical range in the ratio panels are outside the fit region and do not contribute to the fit quality.

to construct the envelope allows one to take into account any residual S_T noninvariance in the systematic uncertainty in the background prediction. We observe a good closure of the method to predict the background distributions in simulated QCD multijet events.

The best fits (taking into account the F-test criterion [82] within each set of nested functions) to the $N = 3$ and $N = 4$ distributions in data, along with the corresponding uncertainty envelopes, are shown in the two panels of figure 3. In both cases, the best fit function is $f(x) = p_0(1 - x^{1/3})^{p_1}/(x^{p_2+p_3\log^2(x)})$, where $x = S_T/\sqrt{s} = S_T/(13\,\text{TeV})$ and p_i are the four free parameters of the fit. The envelope of the predictions at large S_T ($S_T > 5.5\,\text{TeV}$, most relevant for the present search) is given by the fit with the following 5-parameter function: $\phi(x) = p_0(1-x)^{p_1}/(x^{p_2+p_3\log(x)+p_4\log^2(x)})$ to the $N = 4$ (upper edge of the envelope) or $N = 3$ (lower edge of the envelope) distributions. For S_T values below 5.5 TeV the envelope is built piecewise from other template functions fitted to either the $N = 3$ or $N = 4$ distribution.

6.3 Background normalization

The next step in the background estimation for various inclusive multiplicities is to normalize the template and the uncertainty envelope, obtained as described above, to low-S_T data for various inclusive multiplicities. This has to be done with care, as the S_T invariance is only expected to be observed above a certain threshold, which depends on the inclusive multiplicity requirement. Indeed, since there is a p_T threshold on the objects whose transverse energies count toward the S_T value, the minimum possible S_T value depends on the number of objects in the final state, and therefore the shape invariance for an S_T spectrum with $N \geq N^{\text{min}}$ is only observed above a certain S_T threshold, which increases with N^{min}. In order to determine the minimum value of S_T for which this invariance holds, we find a plateau in the ratio of the S_T spectrum for each inclusive multiplicity to that for $N = 3$ in simulated multijet events. The plateau for each multiplicity is found by fitting the ratio

JHEP11(2018)042

Multiplicity	99% turn-on point (TeV)	Normalization region (TeV)	Normalization scale factor (data)
$\geq$3	2.44 ± 0.06	2.5–2.9	3.437 ± 0.025
$\geq$4	2.47 ± 0.06	2.5–2.9	2.437 ± 0.019
$\geq$5	2.60 ± 0.07	2.7–3.1	1.379 ± 0.016
$\geq$6	2.75 ± 0.11	2.9–3.3	0.652 ± 0.012
$\geq$7	2.98 ± 0.13	3.0–3.4	0.516 ± 0.015
$\geq$8	3.18 ± 0.21	3.2–3.6	0.186 ± 0.011
$\geq$9	3.25 ± 0.28	3.2–3.6	0.055 ± 0.006
$\geq$10	3.02 ± 0.26	3.2–3.6	0.012 ± 0.003
$\geq$11	2.89 ± 0.24	3.2–3.6	0.002 ± 0.001

Table 3. The S_{T} invariance thresholds from fits to simulated QCD multijet background spectra, normalization region definitions, and normalization scale factors in data for different inclusive multiplicities.

with a sigmoid function. The lower bound of the normalization region (NR) is chosen to be above the 99% point of the corresponding sigmoid function. The upper bound of each NR is chosen to be 0.4 TeV above the corresponding lower bound to ensure sufficient event count in the NR. Since the size of the simulated QCD multijet background sample is not sufficient to reliably extract the turn-on threshold for inclusive multiplicities of $N \geq 9$–11, for these multiplicities we use the same NR as for the $N \geq 8$ distribution. A self-consistency check with the CMS data sample has shown that this procedure provides an adequate description of the data. Table 3 summarizes the turn-on thresholds and the NR boundaries obtained for each inclusive multiplicity.

The normalization scale factors are calculated as the ratio of the number of events in each NR for the inclusive multiplicities of $N \geq 3, \ldots, 11$ to that for the exclusive multiplicity of $N = 3$ in data, and are listed in table 3. The relative scale factor uncertainties are derived from the number of events in each NR, as $1/\sqrt{N_{\mathrm{NR}}}$, where N_{NR} is the number of events in the corresponding NR.

6.4 Comparison with data

The results of the background prediction and their comparison with the observed data are shown in figures 4 and 5 for inclusive multiplicities $N \geq 3, \ldots, 11$. The data are consistent with the background predictions in the entire S_{T} range probed, for all inclusive multiplicities.

7 Systematic uncertainties

There are several sources of systematic uncertainty in this analysis. Since the background estimation is based on control samples in data, the only uncertainties affecting the back-

JHEP11(2018)042

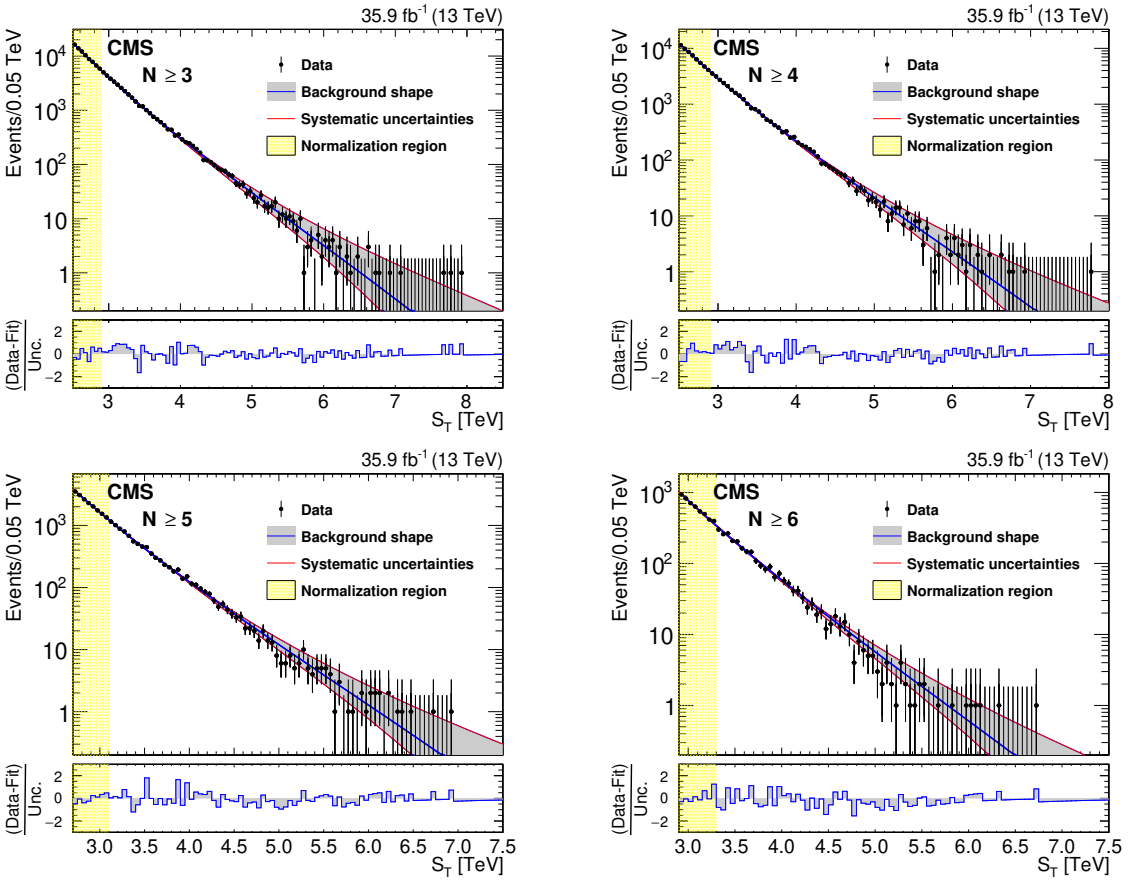

Figure 4. The comparison of data and the background predictions after the normalization for inclusive multiplicities $N \geq 3, \ldots, 6$ (left to right, upper to lower). The gray band shows the background shape uncertainty alone and the red lines also include the normalization uncertainty. The bottom panels show the difference between the data and the background prediction from the fit, divided by the overall uncertainty, which includes the statistical uncertainty of data as well as the shape and normalization uncertainties in the background prediction, added in quadrature.

ground predictions are the modeling of the background shape via template functions and the normalization of the chosen function to data at low S_T, as described in section 6. They are found to be 1–130% and 0.7–50%, depending on the values of S_T and N^{min}, respectively.

For the signal, we consider the uncertainties in the PDFs, jet energy scale (JES), and the integrated luminosity. For the PDF uncertainty, we only consider the effect on the signal acceptance, while the PDF uncertainty in the signal cross section is treated as a part of the theoretical uncertainty and therefore is not propagated in the experimental cross section limit. The uncertainty in the signal acceptance is calculated using PDF4LHC recommendations [83, 84] based on the quadratic sum of variations from the MSTW2008 uncertainty set (≈0.5%), as well as the variations obtained by using three different PDF sets: MSTW2008, CTEQ6.1 [85], and NNPDF2.3 [76] (up to 6% based on the difference between the default and CTEQ6.1 sets) for one of the benchmark models (nonrotating BH with $M_D = 3\,\text{TeV}$, $M_{BH} = 5.5\,\text{TeV}$, and $n = 2$, as generated by BlackMax); the size of

JHEP11(2018)042

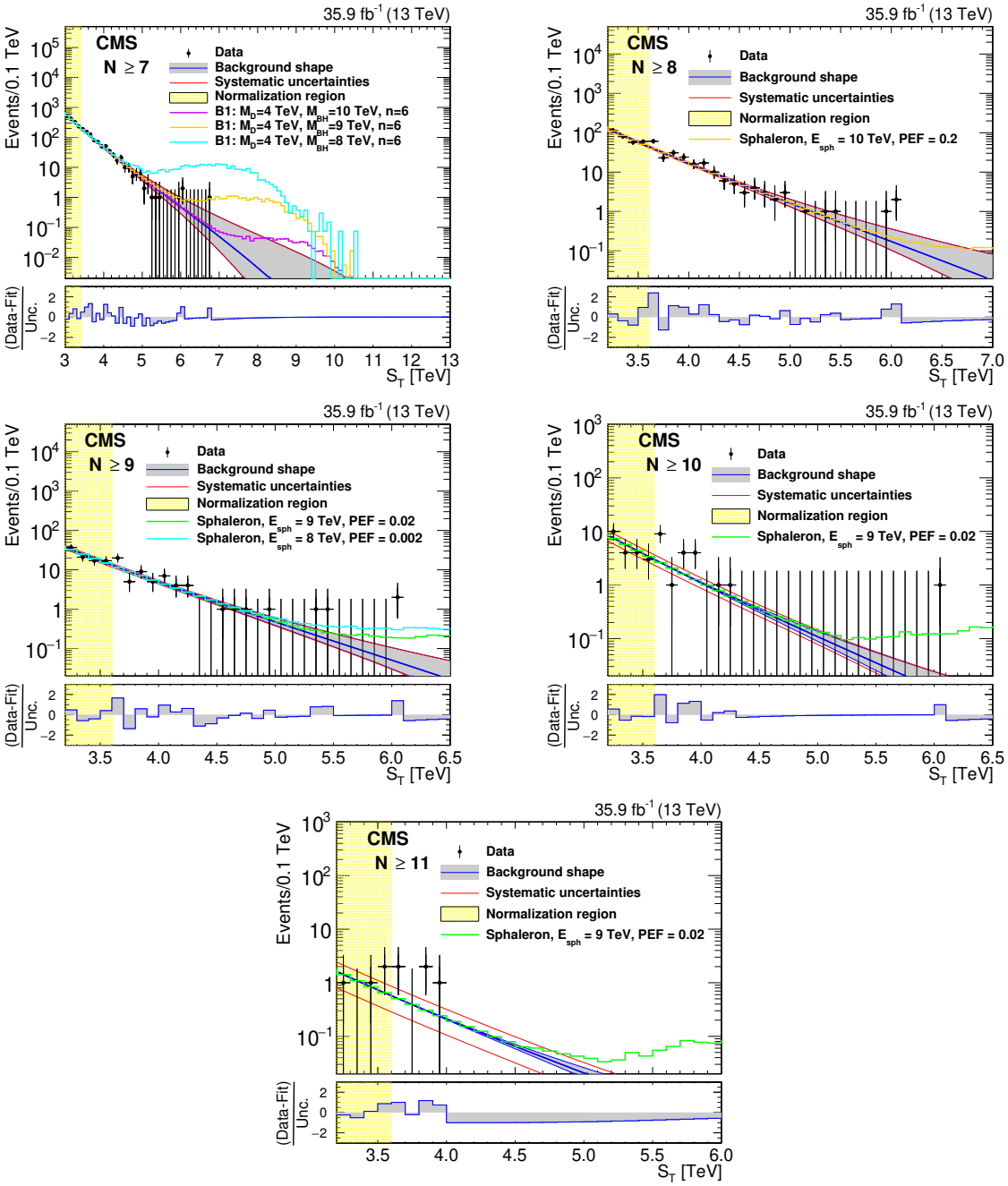

Figure 5. The comparison of data and the background predictions after normalization for inclusive multiplicities of $N \geq 7, \ldots, 11$ (left to right, upper to lower). The gray band shows the shape uncertainty and the red lines also include the normalization uncertainty. The bottom panels show the difference between the data and the background prediction from the fit, divided by the overall uncertainty, which includes the statistical uncertainty of data as well as the shape and normalization uncertainties in the background prediction, added in quadrature. The $N \geq 7$ ($N \geq 8, \ldots, 11$) distributions also show contributions from benchmark BlackMax B1 (sphaleron) signals added to the expected background.

JHEP11(2018)042

Uncertainty source	Effect on signal acceptance	Effect on background
PDF	±6%	—
JES	±5%	—
Integrated luminosity	±2.5%	—
Shape modeling	—	±(1–130)%, depending on S_T
Normalization	—	±(0.7–50)%, depending on N^{min}

Table 4. Summary of systematic uncertainties in the signal acceptance and the background estimate.

the effect for other benchmark points is similar. To be conservative, we assign a systematic uncertainty of 6% due to the choice of PDFs for all signal samples. The JES uncertainty affects the signal acceptance because of the kinematic requirements on the objects and the fraction of signal events passing a certain S_T^{min} threshold used for limit setting, as described in section 8. In order to account for these effects, the jet four-momenta are simultaneously shifted up or down by the JES uncertainty, which is a function of the jet p_T and η, and the largest of the two differences with respect to the use of the nominal JES is assigned as the uncertainty. The uncertainty due to JES depends on M_{BH} and varies between <1 and 5%; we conservatively assign a constant value of 5% as the signal acceptance uncertainty due to JES. Finally, the integrated luminosity is measured with an uncertainty of 2.5% [86]. Effects of all other uncertainties on the signal acceptance are negligible.

The values of systematic uncertainties that are used in this analysis are summarized in table 4.

8 Results

As shown in figures 4 and 5, there is no evidence for a statistically significant signal observed in any of the inclusive S_T distributions. The null results of the search are interpreted in terms of model-independent limits on BSM physics in energetic, multiparticle final states, and as model-specific limits for a set of semiclassical BH and SB scenarios, as well as for EW sphalerons.

Limits are set using the CL_s method [87–89] with log-normal priors in the likelihood to constrain the nuisance parameters near their best estimated values. We do not use an asymptotic approximation of the CL_s method [90], as for most of the models the optimal search region corresponds to a very low background expectation, in which case the asymptotic approximation is known to overestimate the search sensitivity.

8.1 Model-independent limits

The main result of this analysis is a set of model-independent upper limits on the product of signal cross section and acceptance (σA) in inclusive $N \geq N^{min}$ final states, as a function of the minimum S_T requirement, S_T^{min}, obtained from a simple counting experiment for $S_T > S_T^{min}$. These limits can then be translated into limits on the M_{BH}^{min} in a variety of models,

JHEP11(2018)042

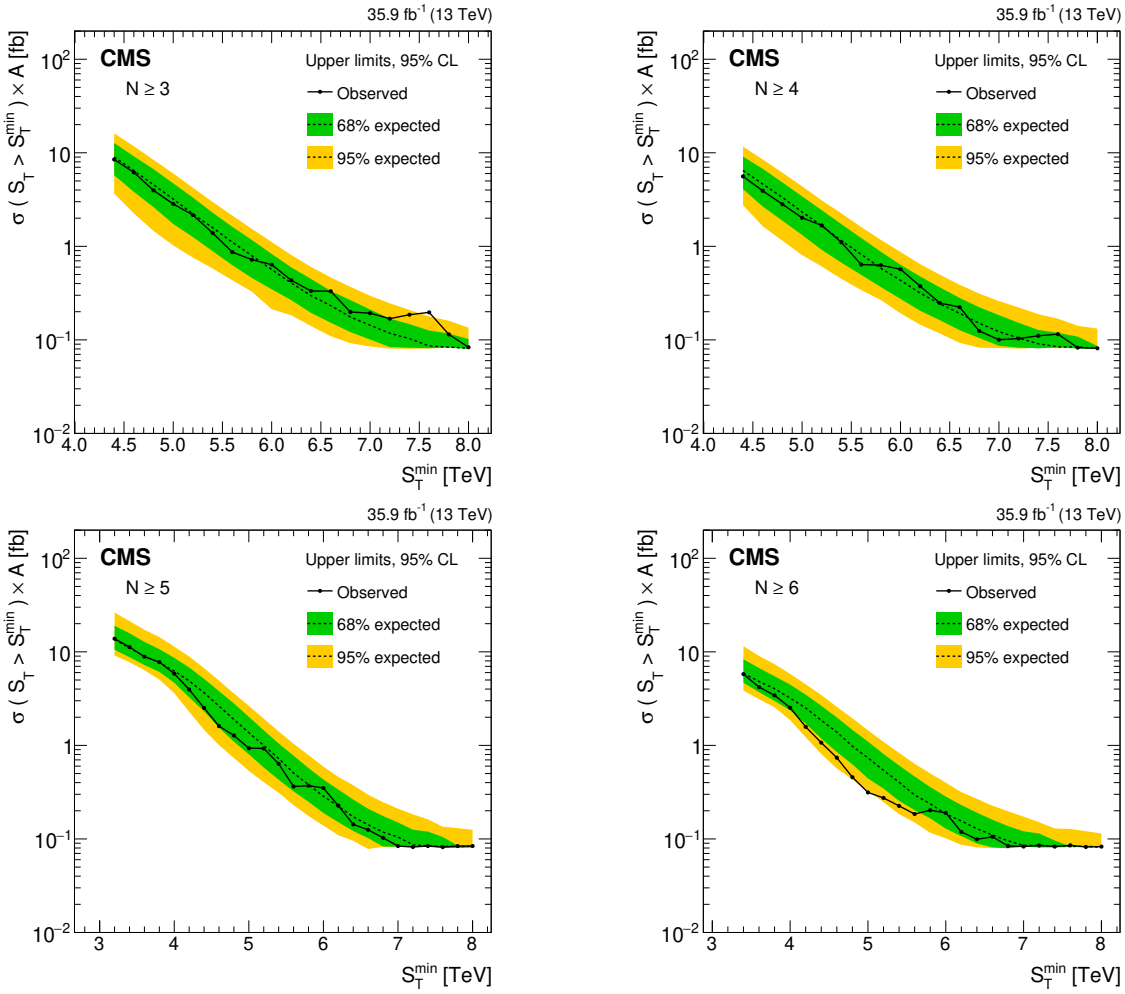

Figure 6. Model-independent upper limits on the cross section times acceptance for four sets of inclusive multiplicity thresholds, $N \geq 3, \ldots, 6$ (left to right, upper to lower). Observed (expected) limits are shown as the black solid (dotted) lines. The inner (outer) band represents the ± 1 (± 2) standard deviation uncertainty in the expected limit.

or on any other signals resulting in an energetic, multi-object final state. We start with the limits for the inclusive multiplicities $N \geq 3, 4$, which can be used to constrain models resulting in lower multiplicities of the final-state objects. Since part of the data entering these distributions are used to determine the background shape and its uncertainties, the limits are set only for $S_{\mathrm{T}}^{\mathrm{min}}$ values above the background fit region, i.e., for $S_{\mathrm{T}} > 4.5\,\mathrm{TeV}$. For other multiplicities, the limits are shown for S_{T} values above the NRs listed in table 3. These limits at 95% confidence level (CL) are shown in figures 6 and 7. When computing the limits, we use systematic uncertainties in the signal acceptance applicable to the specific models discussed in this paper, as documented in section 7. It is reasonable to expect these limits to apply to a large variety of models resulting in multi-object final states dominated by jets. The limits on the product of the cross section and acceptance approach 0.08 fb at high values of $S_{\mathrm{T}}^{\mathrm{min}}$.

JHEP11(2018)042

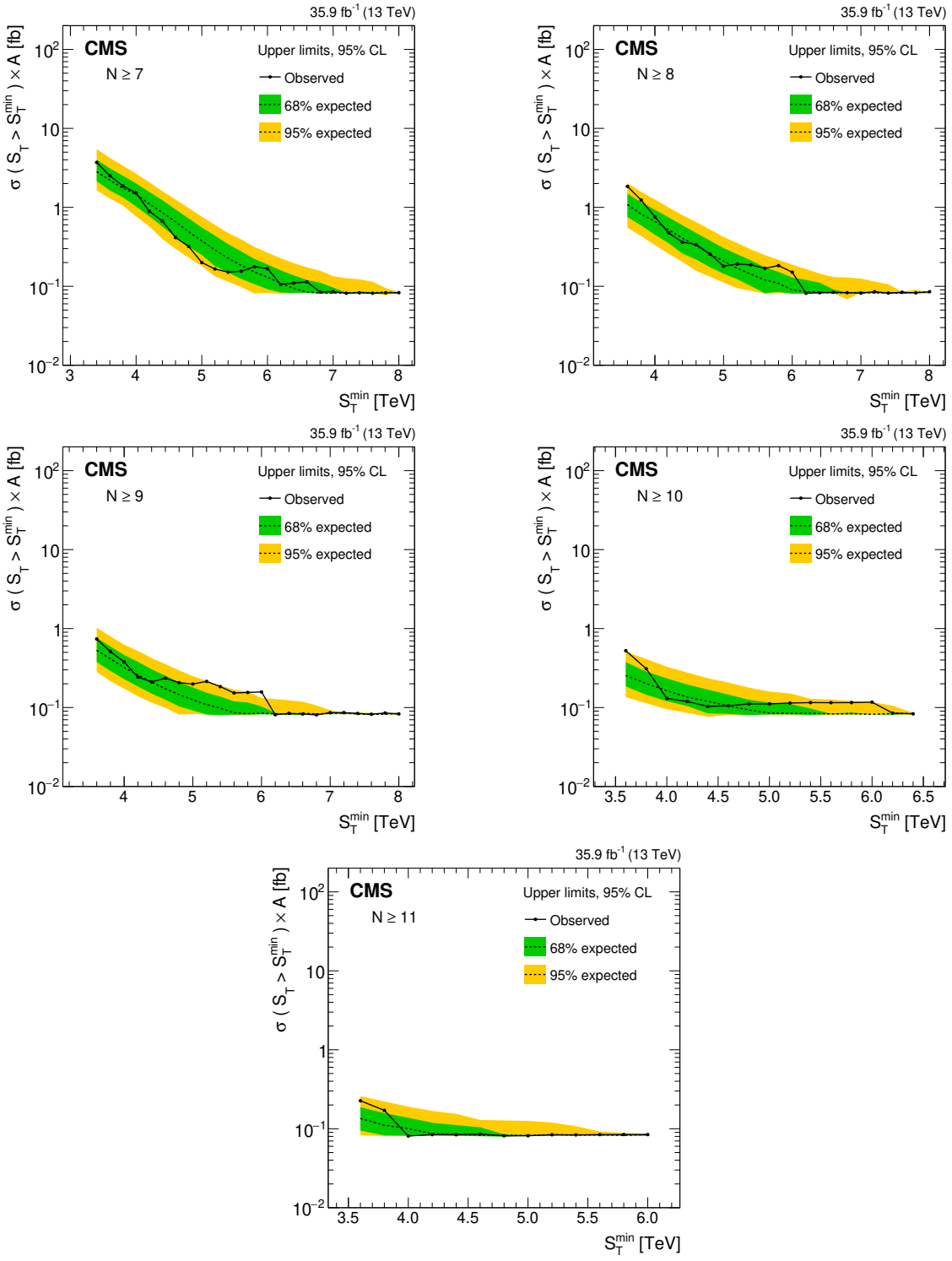

Figure 7. Model-independent upper limits on the cross section times acceptance for five sets of inclusive multiplicity thresholds, $N \geq 7, \ldots, 11$ (left to right, upper to lower). Observed (expected) limits are shown as the black solid (dotted) lines. The inner (outer) band represents the ± 1 (± 2) standard deviation uncertainty in the expected limit.

JHEP11(2018)042

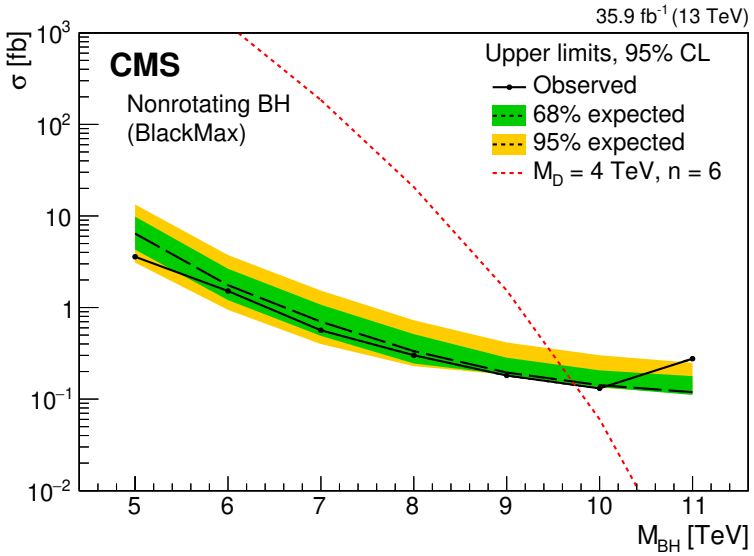

Figure 8. Example of a model-specific limit on $M_{\mathrm{BH}}^{\mathrm{min}}$ for a semiclassical nonrotating BH model (BlackMax point B1) with $M_{\mathrm{D}} = 4\,\mathrm{TeV}$ $n_{\mathrm{ED}} = 6$, as a function of $M_{\mathrm{BH}}^{\mathrm{min}}$. The 95% CL upper exclusion limit on the signal cross section for each $M_{\mathrm{BH}}^{\mathrm{min}}$ value is obtained at the optimal $(N^{\mathrm{min}}, S_{\mathrm{T}}^{\mathrm{min}})$ point, which ranges from $(7, 5.0\,\mathrm{TeV})$ for $M_{\mathrm{BH}}^{\mathrm{min}} = 5\,\mathrm{TeV}$ to $(3, 7.6\,\mathrm{TeV})$ for $M_{\mathrm{BH}}^{\mathrm{min}} = 11\,\mathrm{TeV}$. Also shown with a dashed line are the theoretical cross sections corresponding to these optimal points. The inner (outer) band represents the ±1 (±2) standard deviation uncertainty in the expected limit.

8.2 Model-specific limits

To determine the optimal point of $S_{\mathrm{T}}^{\mathrm{min}}$ and the minimum multiplicity of the final-state objects N^{min} for setting an exclusion limit for a particular model, we calculate the acceptance and the expected limit on the cross section for a given model for each point of the model-independent limit curves, for all inclusive multiplicities. The optimal point of $(N^{\mathrm{min}}, S_{\mathrm{T}}^{\mathrm{min}})$ is chosen as the point that gives the lowest expected cross section limit. In most of the cases this point also maximizes the significance of an observation, for the case of a nonzero signal present in data [36].

An example of a model-specific limit is given in figure 8 for a BlackMax benchmark point B1 (nonrotating semiclassical BH) with $M_{\mathrm{D}} = 4\,\mathrm{TeV}$, $n_{\mathrm{ED}} = 6$, and $M_{\mathrm{BH}}^{\mathrm{min}}$ between 5 and 11 TeV. In this case, the optimal inclusive multiplicity N^{min} starts at 7 for the lowest $M_{\mathrm{BH}}^{\mathrm{min}}$ value of 5 TeV, with the corresponding $S_{\mathrm{T}}^{\mathrm{min}} = 5\,\mathrm{TeV}$. As $M_{\mathrm{BH}}^{\mathrm{min}}$ increases, the optimal point shifts to lower inclusive multiplicities and the corresponding $S_{\mathrm{T}}^{\mathrm{min}}$ increases, reaching $(3, 7.6\,\mathrm{TeV})$ for $M_{\mathrm{BH}}^{\mathrm{min}} = 11\,\mathrm{TeV}$. The corresponding 95% CL upper limit curve and the theoretical cross section for the chosen benchmark point is shown in figure 8. The observed (expected) 95% CL lower limit on $M_{\mathrm{BH}}^{\mathrm{min}}$ in this benchmark model can be read from this plot as the intersection of the theoretical curve with the observed (expected) 95% CL upper limit on the cross section, and is found to be 9.7 (9.7) TeV.

We repeat the above procedure for all chosen benchmark scenarios of semiclassical BHs, listed in tables 1 and 2. The resulting observed limits on the $M_{\mathrm{BH}}^{\mathrm{min}}$ are shown in

JHEP11(2018)042

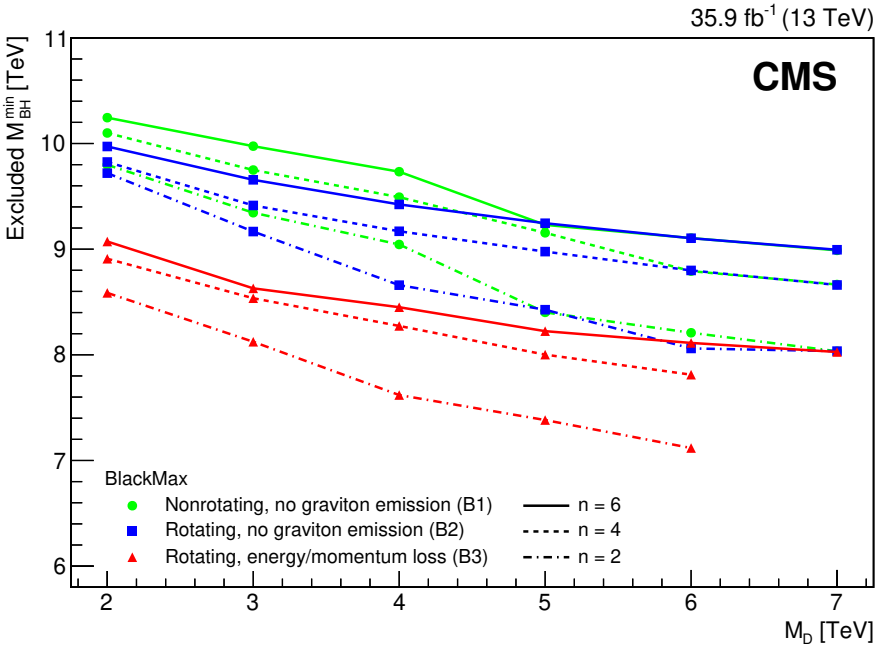

Figure 9. The observed 95% CL lower limits on $M_{\mathrm{BH}}^{\mathrm{min}}$ as a function of M_{D} at different n for the models B1–B3 generated with BlackMax.

figures 9 and 10, for the BlackMax and charybdis 2 benchmarks, respectively. We also obtain similar limits on the SB mass for the set of the SB model parameters we scanned. These limits are shown in figure 11 for a fixed string scale $M_{\mathrm{S}} = 3.6\,\mathrm{TeV}$, as a function of the string coupling g_{S} (left plot) and for a fixed string coupling $g_{\mathrm{S}} = 0.2$ as a function of the string scale M_{S} (right plot). The search excludes SB masses below 7.1–9.4 TeV, depending on the values of the string scale and coupling.

For the sphaleron signal, the optimal $(N^{\mathrm{min}}, S_{\mathrm{T}}^{\mathrm{min}})$ point is also chosen by scanning for the lowest expected limit and is found to be $(8, 6.2\,\mathrm{TeV})$ for $E_{\mathrm{sph}} = 9$ and 10 TeV, and $(9, 5.6\,\mathrm{TeV})$ for $E_{\mathrm{sph}} = 8\,\mathrm{TeV}$. Consequently, the exclusion limit on the sphaleron cross section can be converted into a limit on the PEF, defined in section 5.2. Following ref. [49] we calculate the PEF limits for the nominal $E_{\mathrm{sph}} = 9\,\mathrm{TeV}$, as well as for the modified values of $E_{\mathrm{sph}} = 8$ and 10 TeV. The observed and expected 95% CL upper limits on the PEF are shown in figure 12. The observed (expected) limit obtained for the nominal $E_{\mathrm{sph}} = 9\,\mathrm{TeV}$ is 0.021 (0.012), which is an order of magnitude more stringent than the limit obtained in ref. [49] based on the reinterpretation of the ATLAS result [34].

9 Summary

A search has been presented for generic signals of beyond the standard model physics resulting in energetic multi-object final states, such as would be produced by semiclassical black holes, string balls, and electroweak sphalerons. The search was based on proton-proton collision data at a center-of-mass energy of 13 TeV, collected with the CMS detector

JHEP11(2018)042

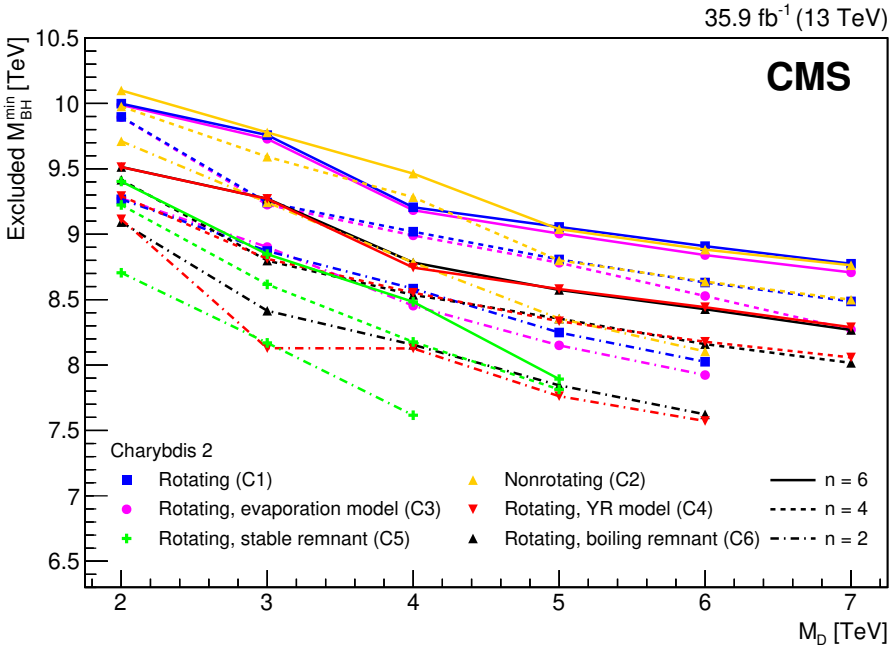

Figure 10. The 95% observed CL lower limits on $M_{\mathrm{BH}}^{\mathrm{min}}$ as a function of M_{D} at different n for the models C1–C6 generated with CHARYBDIS 2.

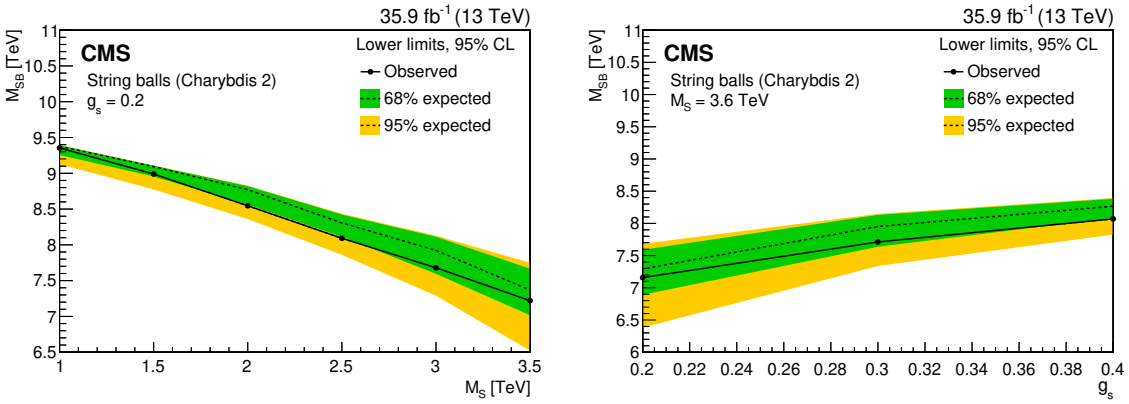

Figure 11. The 95% CL lower limits on a string ball mass as a function of the string scale M_{S} for a fixed value of the string coupling $g_{\mathrm{S}} = 0.2$ (left) and as a function of the string coupling g_{S} for a fixed value of the string scale $M_{\mathrm{S}} = 3.6\,\mathrm{TeV}$ (right). The inner (outer) band represents the ± 1 (± 2) standard deviation uncertainty in the expected limit. The area below the solid curve is excluded by this search.

JHEP11(2018)042

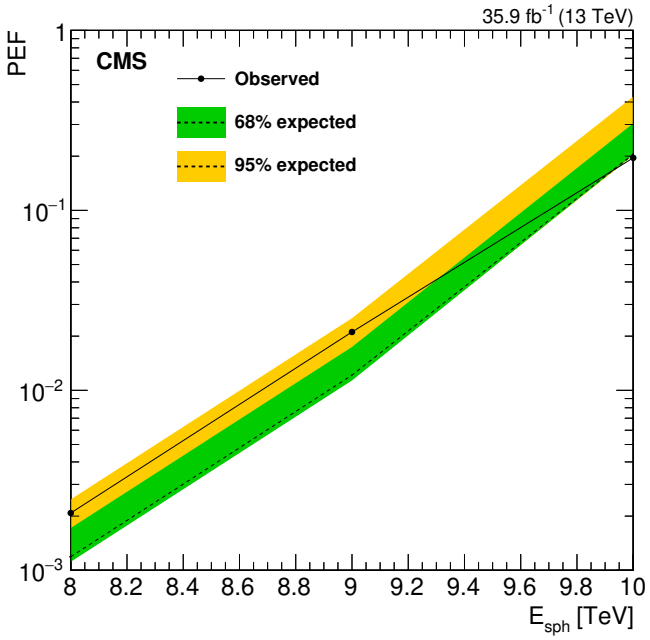

Figure 12. Observed (solid curve) and expected (dashed black curve) 95% CL upper limit on the pre-exponential factor PEF of the sphaleron production as a function of E_{sph}. The inner (outer) band represents the ± 1 (± 2) standard deviation uncertainty in the expected limit. The area above the solid curve is excluded by this search.

in 2016 and corresponding to an integrated luminosity of $35.9\,\text{fb}^{-1}$. The background, dominated by QCD multijet production, is determined solely from low-multiplicity samples in data. Comparing the distribution of the total transverse momentum S_{T} of the final-state objects in data with that expected from the backgrounds, we set 95% confidence level model-independent upper limits on the product of the production cross section and acceptance for such final states, as a function of the minimum S_{T} for minimum final-state multiplicities between 3 and 11. These limits reach 0.08 fb at high S_{T} thresholds. By calculating the acceptance values for benchmark black hole, string ball, and sphaleron signal models, we convert these model-independent limits into lower limits on the minimum semiclassical black hole mass and string ball mass. The limits extend as high as 10.1 TeV, thus improving significantly on previous results. We have also set the first experimental upper limit on the electroweak sphaleron pre-exponential factor of 0.021 for the sphaleron transition energy of 9 TeV.

Acknowledgments

We congratulate our colleagues in the CERN accelerator departments for the excellent performance of the LHC and thank the technical and administrative staffs at CERN and at other CMS institutes for their contributions to the success of the CMS effort. In addition, we gratefully acknowledge the computing centers and personnel of the Worldwide LHC Computing Grid for delivering so effectively the computing infrastructure essential to our

JHEP11(2018)042

analyses. Finally, we acknowledge the enduring support for the construction and operation of the LHC and the CMS detector provided by the following funding agencies: BMBWF and FWF (Austria); FNRS and FWO (Belgium); CNPq, CAPES, FAPERJ, FAPERGS, and FAPESP (Brazil); MES (Bulgaria); CERN; CAS, MoST, and NSFC (China); COLCIENCIAS (Colombia); MSES and CSF (Croatia); RPF (Cyprus); SENESCYT (Ecuador); MoER, ERC IUT, and ERDF (Estonia); Academy of Finland, MEC, and HIP (Finland); CEA and CNRS/IN2P3 (France); BMBF, DFG, and HGF (Germany); GSRT (Greece); NKFIA (Hungary); DAE and DST (India); IPM (Iran); SFI (Ireland); INFN (Italy); MSIP and NRF (Republic of Korea); MES (Latvia); LAS (Lithuania); MOE and UM (Malaysia); BUAP, CINVESTAV, CONACYT, LNS, SEP, and UASLP-FAI (Mexico); MOS (Montenegro); MBIE (New Zealand); PAEC (Pakistan); MSHE and NSC (Poland); FCT (Portugal); JINR (Dubna); MON, RosAtom, RAS, RFBR, and NRC KI (Russia); MESTD (Serbia); SEIDI, CPAN, PCTI, and FEDER (Spain); MOSTR (Sri Lanka); Swiss Funding Agencies (Switzerland); MST (Taipei); ThEPCenter, IPST, STAR, and NSTDA (Thailand); TUBITAK and TAEK (Turkey); NASU and SFFR (Ukraine); STFC (United Kingdom); DOE and NSF (U.S.A.).

Individuals have received support from the Marie-Curie program and the European Research Council and Horizon 2020 Grant, contract No. 675440 (European Union); the Leventis Foundation; the A. P. Sloan Foundation; the Alexander von Humboldt Foundation; the Belgian Federal Science Policy Office; the Fonds pour la Formation à la Recherche dans l'Industrie et dans l'Agriculture (FRIA-Belgium); the Agentschap voor Innovatie door Wetenschap en Technologie (IWT-Belgium); the F.R.S.-FNRS and FWO (Belgium) under the "Excellence of Science — EOS" — be.h project n. 30820817; the Ministry of Education, Youth and Sports (MEYS) of the Czech Republic; the Lendület ("Momentum") Programme and the János Bolyai Research Scholarship of the Hungarian Academy of Sciences, the New National Excellence Program ÚNKP, the NKFIA research grants 123842, 123959, 124845, 124850 and 125105 (Hungary); the Council of Science and Industrial Research, India; the HOMING PLUS program of the Foundation for Polish Science, cofinanced from European Union, Regional Development Fund, the Mobility Plus programme of the Ministry of Science and Higher Education, the National Science Center (Poland), contracts Harmonia 2014/14/M/ST2/00428, Opus 2014/13/B/ST2/02543, 2014/15/B/ST2/03998, and 2015/19/B/ST2/02861, Sonata-bis 2012/07/E/ST2/01406; the National Priorities Research Program by Qatar National Research Fund; the Programa Estatal de Fomento de la Investigación Científica y Técnica de Excelencia María de Maeztu, grant MDM-2015-0509 and the Programa Severo Ochoa del Principado de Asturias; the Thalis and Aristeia programmes cofinanced by EU-ESF and the Greek NSRF; the Rachadapisek Sompot Fund for Postdoctoral Fellowship, Chulalongkorn University and the Chulalongkorn Academic into Its 2nd Century Project Advancement Project (Thailand); the Welch Foundation, contract C-1845; and the Weston Havens Foundation (U.S.A.).

JHEP11(2018)042

References

[1] S.L. Glashow, *Partial-symmetries of weak interactions*, *Nucl. Phys.* **22** (1961) 579.

[2] S. Weinberg, *A model of leptons*, *Phys. Rev. Lett.* **19** (1967) 1264 [INSPIRE].

[3] A. Salam, *Weak and electromagnetic interactions*, in *Elementary particle physics: relativistic groups and analyticity. Proceedings of the eighth Nobel symposium*, N. Svartholm ed., Almqvist & Wiksell, Stockholm, Sweden, (1968), pg. 367 [INSPIRE].

[4] P. Ramond, *Dual theory for free fermions*, *Phys. Rev.* **D 3** (1971) 2415 [INSPIRE].

[5] Yu. A. Golfand and E.P. Likhtman, *Extension of the algebra of Poincaré group generators and violation of p invariance*, *JETP Lett.* **13** (1971) 323 [*Pisma Zh. Eksp. Teor. Fiz.* **13** (1971) 452] [INSPIRE].

[6] A. Neveu and J.H. Schwarz, *Factorizable dual model of pions*, *Nucl. Phys.* **B 31** (1971) 86 [INSPIRE].

[7] D.V. Volkov and V.P. Akulov, *Possible universal neutrino interaction*, *JETP Lett.* **16** (1972) 438 [*Pisma Zh. Eksp. Teor. Fiz.* **16** (1972) 621] [INSPIRE].

[8] J. Wess and B. Zumino, *A Lagrangian model invariant under supergauge transformations*, *Phys. Lett.* **B 49** (1974) 52 [INSPIRE].

[9] J. Wess and B. Zumino, *Supergauge transformations in four-dimensions*, *Nucl. Phys.* **B 70** (1974) 39 [INSPIRE].

[10] P. Fayet, *Supergauge invariant extension of the Higgs mechanism and a model for the electron and its neutrino*, *Nucl. Phys.* **B 90** (1975) 104 [INSPIRE].

[11] H.P. Nilles, *Supersymmetry, supergravity and particle physics*, *Phys. Rept.* **110** (1984) 1 [INSPIRE].

[12] G.R. Farrar and P. Fayet, *Phenomenology of the production, decay and detection of new hadronic states associated with supersymmetry*, *Phys. Lett.* **B 76** (1978) 575 [INSPIRE].

[13] N. Arkani-Hamed, S. Dimopoulos and G.R. Dvali, *The hierarchy problem and new dimensions at a millimeter*, *Phys. Lett.* **B 429** (1998) 263 [hep-ph/9803315] [INSPIRE].

[14] I. Antoniadis, N. Arkani-Hamed, S. Dimopoulos and G.R. Dvali, *New dimensions at a millimeter to a Fermi and superstrings at a TeV*, *Phys. Lett.* **B 436** (1998) 257 [hep-ph/9804398] [INSPIRE].

[15] N. Arkani-Hamed, S. Dimopoulos and G.R. Dvali, *Phenomenology, astrophysics and cosmology of theories with submillimeter dimensions and TeV scale quantum gravity*, *Phys. Rev.* **D 59** (1999) 086004 [hep-ph/9807344] [INSPIRE].

[16] L. Randall and R. Sundrum, *A large mass hierarchy from a small extra dimension*, *Phys. Rev. Lett.* **83** (1999) 3370 [hep-ph/9905221] [INSPIRE].

[17] L. Randall and R. Sundrum, *An alternative to compactification*, *Phys. Rev. Lett.* **83** (1999) 4690 [hep-th/9906064] [INSPIRE].

[18] ATLAS collaboration, *Observation of a new particle in the search for the Standard Model Higgs boson with the ATLAS detector at the LHC*, *Phys. Lett.* **B 716** (2012) 1 [arXiv:1207.7214] [INSPIRE].

[19] CMS collaboration, *Observation of a new boson at a mass of* 125 *GeV with the CMS experiment at the LHC*, *Phys. Lett.* **B 716** (2012) 30 [arXiv:1207.7235] [INSPIRE].

JHEP11(2018)042

[20] CMS collaboration, *Observation of a new boson with mass near 125 GeV in pp collisions at $\sqrt{s} = 7$ and 8 TeV*, *JHEP* **06** (2013) 081 [arXiv:1303.4571] [INSPIRE].

[21] ATLAS and CMS collaborations, *Combined measurement of the Higgs boson mass in pp collisions at $\sqrt{s} = 7$ and 8 TeV with the ATLAS and CMS experiments*, *Phys. Rev. Lett.* **114** (2015) 191803 [arXiv:1503.07589] [INSPIRE].

[22] CMS collaboration, *Measurements of properties of the Higgs boson decaying into the four-lepton final state in pp collisions at $\sqrt{s} = 13$ TeV*, *JHEP* **11** (2017) 047 [arXiv:1706.09936] [INSPIRE].

[23] R. Barbieri and G.F. Giudice, *Upper bounds on supersymmetric particle masses*, *Nucl. Phys.* **B 306** (1988) 63 [INSPIRE].

[24] S. Dimopoulos and L. Susskind, *Mass without scalars*, *Nucl. Phys.* **B 155** (1979) 237 [INSPIRE].

[25] S. Dimopoulos and G.L. Landsberg, *Black holes at the LHC*, *Phys. Rev. Lett.* **87** (2001) 161602 [hep-ph/0106295] [INSPIRE].

[26] S.B. Giddings and S.D. Thomas, *High-energy colliders as black hole factories: the end of short distance physics*, *Phys. Rev.* **D 65** (2002) 056010 [hep-ph/0106219] [INSPIRE].

[27] S.W. Hawking, *Particle creation by black holes*, *Commun. Math. Phys.* **43** (1975) 199 [*Erratum ibid.* **46** (1976) 206] [INSPIRE].

[28] X. Calmet, W. Gong and S.D.H. Hsu, *Colorful quantum black holes at the LHC*, *Phys. Lett.* **B 668** (2008) 20 [arXiv:0806.4605] [INSPIRE].

[29] D.M. Gingrich, *Quantum black holes with charge, colour and spin at the LHC*, *J. Phys.* **G 37** (2010) 105008 [arXiv:0912.0826] [INSPIRE].

[30] D.M. Gingrich, *Monte Carlo event generator for black hole production and decay in proton-proton collisions*, *Comput. Phys. Commun.* **181** (2010) 1917 [arXiv:0911.5370] [INSPIRE].

[31] S. Dimopoulos and R. Emparan, *String balls at the LHC and beyond*, *Phys. Lett.* **B 526** (2002) 393 [hep-ph/0108060] [INSPIRE].

[32] R. Hagedorn, *Statistical thermodynamics of strong interactions at high-energies*, *Nuovo Cim. Suppl.* **3** (1965) 147 [INSPIRE].

[33] G. Landsberg, *Black holes at the Large Hadron Collider*, *Fundam. Theor. Phys.* **178** (2015) 267 [INSPIRE].

[34] ATLAS collaboration, *Search for strong gravity in multijet final states produced in pp collisions at $\sqrt{s} = 13$ TeV using the ATLAS detector at the LHC*, *JHEP* **03** (2016) 026 [arXiv:1512.02586] [INSPIRE].

[35] ATLAS collaboration, *Search for TeV-scale gravity signatures in high-mass final states with leptons and jets with the ATLAS detector at $\sqrt{s} = 13$ TeV*, *Phys. Lett.* **B 760** (2016) 520 [arXiv:1606.02265] [INSPIRE].

[36] CMS collaboration, *Search for black holes in high-multiplicity final states in proton-proton collisions at $\sqrt{s} = 13$ TeV*, *Phys. Lett.* **B 774** (2017) 279 [arXiv:1705.01403] [INSPIRE].

[37] ATLAS collaboration, *Search for new phenomena in dijet mass and angular distributions from pp collisions at $\sqrt{s} = 13$ TeV with the ATLAS detector*, *Phys. Lett.* **B 754** (2016) 302 [arXiv:1512.01530] [INSPIRE].

JHEP11(2018)042

[38] ATLAS collaboration, *Search for new phenomena with photon+jet events in proton-proton collisions at $\sqrt{s} = 13$ TeV with the ATLAS detector*, *JHEP* **03** (2016) 041 [arXiv:1512.05910] [INSPIRE].

[39] CMS collaboration, *Search for new physics with dijet angular distributions in proton-proton collisions at $\sqrt{s} = 13$ TeV*, *JHEP* **07** (2017) 013 [arXiv:1703.09986] [INSPIRE].

[40] ATLAS collaboration, *Search for new phenomena in dijet events using 37 fb^{-1} of pp collision data collected at $\sqrt{s} = 13$ TeV with the ATLAS detector*, *Phys. Rev.* **D 96** (2017) 052004 [arXiv:1703.09127] [INSPIRE].

[41] ATLAS collaboration, *Search for new phenomena in high-mass final states with a photon and a jet from pp collisions at $\sqrt{s} = 13$ TeV with the ATLAS detector*, *Eur. Phys. J.* **C 78** (2018) 102 [arXiv:1709.10440] [INSPIRE].

[42] CMS collaboration, *Search for lepton-flavor violating decays of heavy resonances and quantum black holes to eμ final states in proton-proton collisions at $\sqrt{s} = 13$ TeV*, *JHEP* **04** (2018) 073 [arXiv:1802.01122] [INSPIRE].

[43] G. 't Hooft, *Symmetry breaking through Bell-Jackiw anomalies*, *Phys. Rev. Lett.* **37** (1976) 8 [INSPIRE].

[44] F.R. Klinkhamer and N.S. Manton, *A saddle point solution in the Weinberg-Salam theory*, *Phys. Rev.* **D 30** (1984) 2212 [INSPIRE].

[45] M. Trodden, *Electroweak baryogenesis*, *Rev. Mod. Phys.* **71** (1999) 1463 [hep-ph/9803479] [INSPIRE].

[46] A. Ringwald, *High-energy breakdown of perturbation theory in the electroweak instanton sector*, *Nucl. Phys.* **B 330** (1990) 1 [INSPIRE].

[47] S.-S. Chern and J. Simons, *Characteristic forms and geometric invariants*, *Annals Math.* **99** (1974) 48 [INSPIRE].

[48] S.-H. Henry Tye and S.S.C. Wong, *Bloch wave function for the periodic sphaleron potential and unsuppressed baryon and lepton number violating processes*, *Phys. Rev.* **D 92** (2015) 045005 [arXiv:1505.03690] [INSPIRE].

[49] J. Ellis and K. Sakurai, *Search for sphalerons in proton-proton collisions*, *JHEP* **04** (2016) 086 [arXiv:1601.03654] [INSPIRE].

[50] C. Bravo and J. Hauser, *BaryoGEN, a Monte Carlo generator for sphaleron-like transitions in proton-proton collisions*, *JHEP* **11** (2018) 041 [arXiv:1805.02786] [INSPIRE].

[51] E.W. Kolb and M.S. Turner, *The early universe*, *Front. Phys.* **69** (1990) 1 [ISBN:978-0201626742] [INSPIRE].

[52] CMS collaboration, *The CMS trigger system*, 2017 *JINST* **12** P01020 [arXiv:1609.02366] [INSPIRE].

[53] CMS collaboration, *The CMS experiment at the CERN LHC*, 2008 *JINST* **3** S08004 [INSPIRE].

[54] CMS collaboration, *Particle-flow reconstruction and global event description with the CMS detector*, 2017 *JINST* **12** P10003 [arXiv:1706.04965] [INSPIRE].

[55] M. Cacciari, G.P. Salam and G. Soyez, *The anti-k_t jet clustering algorithm*, *JHEP* **04** (2008) 063 [arXiv:0802.1189] [INSPIRE].

JHEP11(2018)042

[56] M. Cacciari, G.P. Salam and G. Soyez, *FastJet user manual*, *Eur. Phys. J.* **C 72** (2012) 1896 [arXiv:1111.6097] [INSPIRE].

[57] CMS collaboration, *Jet energy scale and resolution in the CMS experiment in pp collisions at 8 TeV*, 2017 *JINST* **12** P02014 [arXiv:1607.03663] [INSPIRE].

[58] CMS collaboration, *Performance of the CMS muon detector and muon reconstruction with proton-proton collisions at* $\sqrt{s} = 13$ *TeV*, 2018 *JINST* **13** P06015 [arXiv:1804.04528] [INSPIRE].

[59] CMS collaboration, *Jet algorithms performance in 13 TeV data*, CMS-PAS-JME-16-003, CERN, Geneva, Switzerland, (2017).

[60] CMS collaboration, *Performance of electron reconstruction and selection with the CMS detector in proton-proton collisions at* $\sqrt{s} = 8$ *TeV*, 2015 *JINST* **10** P06005 [arXiv:1502.02701] [INSPIRE].

[61] CMS collaboration, *Performance of photon reconstruction and identification with the CMS detector in proton-proton collisions at* $\sqrt{s} = 8$ *TeV*, 2015 *JINST* **10** P08010 [arXiv:1502.02702] [INSPIRE].

[62] M. Cacciari and G.P. Salam, *Pileup subtraction using jet areas*, *Phys. Lett.* **B 659** (2008) 119 [arXiv:0707.1378] [INSPIRE].

[63] CMS collaboration, *Search for microscopic black hole signatures at the Large Hadron Collider*, *Phys. Lett.* **B 697** (2011) 434 [arXiv:1012.3375] [INSPIRE].

[64] CMS collaboration, *Search for microscopic black holes in pp collisions at* $\sqrt{s} = 7$ *TeV*, *JHEP* **04** (2012) 061 [arXiv:1202.6396] [INSPIRE].

[65] CMS collaboration, *Search for microscopic black holes in pp collisions at* $\sqrt{s} = 8$ *TeV*, *JHEP* **07** (2013) 178 [arXiv:1303.5338] [INSPIRE].

[66] ATLAS collaboration, *Search for TeV-scale gravity signatures in final states with leptons and jets with the ATLAS detector at* $\sqrt{s} = 7$ *TeV*, *Phys. Lett.* **B 716** (2012) 122 [arXiv:1204.4646] [INSPIRE].

[67] ATLAS collaboration, *Search for microscopic black holes and string balls in final states with leptons and jets with the ATLAS detector at* $\sqrt{s} = 8$ *TeV*, *JHEP* **08** (2014) 103 [arXiv:1405.4254] [INSPIRE].

[68] CMS collaboration, *Search for stealth supersymmetry in events with jets, either photons or leptons and low missing transverse momentum in pp collisions at 8 TeV*, *Phys. Lett.* **B 743** (2015) 503 [arXiv:1411.7255] [INSPIRE].

[69] CMS collaboration, *Search for new phenomena in events with high jet multiplicity and low missing transverse momentum in proton-proton collisions at* $\sqrt{s} = 8$ *TeV*, *Phys. Lett.* **B 770** (2017) 257 [arXiv:1608.01224] [INSPIRE].

[70] D.-C. Dai, G. Starkman, D. Stojkovic, C. Issever, E. Rizvi and J. Tseng, *BlackMax: a black-hole event generator with rotation, recoil, split branes and brane tension*, *Phys. Rev.* **D 77** (2008) 076007 [arXiv:0711.3012] [INSPIRE].

[71] C.M. Harris, P. Richardson and B.R. Webber, *CHARYBDIS: a black hole event generator*, *JHEP* **08** (2003) 033 [hep-ph/0307305] [INSPIRE].

[72] J.A. Frost et al., *Phenomenology of production and decay of spinning extra-dimensional black holes at hadron colliders*, *JHEP* **10** (2009) 014 [arXiv:0904.0979] [INSPIRE].

JHEP11(2018)042

[73] H. Yoshino and V.S. Rychkov, *Improved analysis of black hole formation in high-energy particle collisions*, *Phys. Rev.* **D 71** (2005) 104028 [*Erratum ibid.* **D 77** (2008) 089905] [hep-th/0503171] [INSPIRE].

[74] A.D. Martin, W.J. Stirling, R.S. Thorne and G. Watt, *Parton distributions for the LHC*, *Eur. Phys. J.* **C 63** (2009) 189 [arXiv:0901.0002] [INSPIRE].

[75] A.D. Martin, W.J. Stirling, R.S. Thorne and G. Watt, *Heavy-quark mass dependence in global PDF analyses and 3- and 4-flavour parton distributions*, *Eur. Phys. J.* **C 70** (2010) 51 [arXiv:1007.2624] [INSPIRE].

[76] R.D. Ball et al., *Parton distributions with LHC data*, *Nucl. Phys.* **B 867** (2013) 244 [arXiv:1207.1303] [INSPIRE].

[77] H.-L. Lai et al., *New parton distributions for collider physics*, *Phys. Rev.* **D 82** (2010) 074024 [arXiv:1007.2241] [INSPIRE].

[78] J. Alwall et al., *The automated computation of tree-level and next-to-leading order differential cross sections and their matching to parton shower simulations*, *JHEP* **07** (2014) 079 [arXiv:1405.0301] [INSPIRE].

[79] T. Sjöstrand et al., *An introduction to PYTHIA* 8.2, *Comput. Phys. Commun.* **191** (2015) 159 [arXiv:1410.3012] [INSPIRE].

[80] CMS collaboration, *Event generator tunes obtained from underlying event and multiparton scattering measurements*, *Eur. Phys. J.* **C 76** (2016) 155 [arXiv:1512.00815] [INSPIRE].

[81] GEANT4 collaboration, S. Agostinelli et al., *GEANT4: a simulation toolkit*, *Nucl. Instrum. Meth.* **A 506** (2003) 250 [INSPIRE].

[82] R.A. Fisher, *On the interpretation of χ^2 from contingency tables, and the calculation of p*, *J. Roy. Statist. Soc.* **85** (1922) 87.

[83] S. Alekhin et al., *The PDF4LHC working group interim report*, arXiv:1101.0536 [INSPIRE].

[84] M. Botje et al., *The PDF4LHC working group interim recommendations*, arXiv:1101.0538 [INSPIRE].

[85] P.M. Nadolsky et al., *Implications of CTEQ global analysis for collider observables*, *Phys. Rev.* **D 78** (2008) 013004 [arXiv:0802.0007] [INSPIRE].

[86] CMS collaboration, *CMS luminosity measurements for the* 2016 *data taking period*, CMS-PAS-LUM-17-001, CERN, Geneva, Switzerland, (2017).

[87] T. Junk, *Confidence level computation for combining searches with small statistics*, *Nucl. Instrum. Meth.* **A 434** (1999) 435 [hep-ex/9902006] [INSPIRE].

[88] A.L. Read, *Presentation of search results: the CL_s technique*, *J. Phys.* **G 28** (2002) 2693 [INSPIRE].

[89] ATLAS, CMS collaborations and the LHC Higgs Combination Group, *Procedure for the LHC Higgs boson search combination in Summer* 2011, ATL-PHYS-PUB-2011-011, CERN, Geneva, Switzerland, (2011) [CMS-NOTE-2011-005].

[90] G. Cowan, K. Cranmer, E. Gross and O. Vitells, *Asymptotic formulae for likelihood-based tests of new physics*, *Eur. Phys. J.* **C 71** (2011) 1554 [*Erratum ibid.* **C 73** (2013) 2501] [arXiv:1007.1727] [INSPIRE].

JHEP11(2018)042

The CMS collaboration

Yerevan Physics Institute, Yerevan, Armenia

A.M. Sirunyan, A. Tumasyan

Institut für Hochenergiephysik, Wien, Austria

W. Adam, F. Ambrogi, E. Asilar, T. Bergauer, J. Brandstetter, M. Dragicevic, J. Erö, A. Escalante Del Valle, M. Flechl, R. Frühwirth[1], V.M. Ghete, J. Hrubec, M. Jeitler[1], N. Krammer, I. Krätschmer, D. Liko, T. Madlener, I. Mikulec, N. Rad, H. Rohringer, J. Schieck[1], R. Schöfbeck, M. Spanring, D. Spitzbart, A. Taurok, W. Waltenberger, J. Wittmann, C.-E. Wulz[1], M. Zarucki

Institute for Nuclear Problems, Minsk, Belarus

V. Chekhovsky, V. Mossolov, J. Suarez Gonzalez

Universiteit Antwerpen, Antwerpen, Belgium

E.A. De Wolf, D. Di Croce, X. Janssen, J. Lauwers, M. Pieters, M. Van De Klundert, H. Van Haevermaet, P. Van Mechelen, N. Van Remortel

Vrije Universiteit Brussel, Brussel, Belgium

S. Abu Zeid, F. Blekman, J. D'Hondt, I. De Bruyn, J. De Clercq, K. Deroover, G. Flouris, D. Lontkovskyi, S. Lowette, I. Marchesini, S. Moortgat, L. Moreels, Q. Python, K. Skovpen, S. Tavernier, W. Van Doninck, P. Van Mulders, I. Van Parijs

Université Libre de Bruxelles, Bruxelles, Belgium

D. Beghin, B. Bilin, H. Brun, B. Clerbaux, G. De Lentdecker, H. Delannoy, B. Dorney, G. Fasanella, L. Favart, R. Goldouzian, A. Grebenyuk, A.K. Kalsi, T. Lenzi, J. Luetic, N. Postiau, E. Starling, L. Thomas, C. Vander Velde, P. Vanlaer, D. Vannerom, Q. Wang

Ghent University, Ghent, Belgium

T. Cornelis, D. Dobur, A. Fagot, M. Gul, I. Khvastunov[2], D. Poyraz, C. Roskas, D. Trocino, M. Tytgat, W. Verbeke, B. Vermassen, M. Vit, N. Zaganidis

Université Catholique de Louvain, Louvain-la-Neuve, Belgium

H. Bakhshiansohi, O. Bondu, S. Brochet, G. Bruno, C. Caputo, P. David, C. Delaere, M. Delcourt, B. Francois, A. Giammanco, G. Krintiras, V. Lemaitre, A. Magitteri, A. Mertens, M. Musich, K. Piotrzkowski, A. Saggio, M. Vidal Marono, S. Wertz, J. Zobec

Centro Brasileiro de Pesquisas Fisicas, Rio de Janeiro, Brazil

F.L. Alves, G.A. Alves, L. Brito, M. Correa Martins Junior, G. Correia Silva, C. Hensel, A. Moraes, M.E. Pol, P. Rebello Teles

Universidade do Estado do Rio de Janeiro, Rio de Janeiro, Brazil

E. Belchior Batista Das Chagas, W. Carvalho, J. Chinellato[3], E. Coelho, E.M. Da Costa, G.G. Da Silveira[4], D. De Jesus Damiao, C. De Oliveira Martins, S. Fonseca De Souza, H. Malbouisson, D. Matos Figueiredo, M. Melo De Almeida, C. Mora Herrera, L. Mundim, H. Nogima, W.L. Prado Da Silva, L.J. Sanchez Rosas, A. Santoro, A. Sznajder, M. Thiel, E.J. Tonelli Manganote[3], F. Torres Da Silva De Araujo, A. Vilela Pereira

JHEP11(2018)042

Universidade Estadual Paulista [a], Universidade Federal do ABC [b], São Paulo, Brazil

S. Ahuja[a], C.A. Bernardes[a], L. Calligaris[a], T.R. Fernandez Perez Tomei[a], E.M. Gregores[b], P.G. Mercadante[b], S.F. Novaes[a], SandraS. Padula[a], D. Romero Abad[b]

Institute for Nuclear Research and Nuclear Energy, Bulgarian Academy of Sciences, Sofia, Bulgaria

A. Aleksandrov, R. Hadjiiska, P. Iaydjiev, A. Marinov, M. Misheva, M. Rodozov, M. Shopova, G. Sultanov

University of Sofia, Sofia, Bulgaria

A. Dimitrov, L. Litov, B. Pavlov, P. Petkov

Beihang University, Beijing, China

W. Fang[5], X. Gao[5], L. Yuan

Institute of High Energy Physics, Beijing, China

M. Ahmad, J.G. Bian, G.M. Chen, H.S. Chen, M. Chen, Y. Chen, C.H. Jiang, D. Leggat, H. Liao, Z. Liu, F. Romeo, S.M. Shaheen[6], A. Spiezia, J. Tao, C. Wang, Z. Wang, E. Yazgan, H. Zhang, J. Zhao

State Key Laboratory of Nuclear Physics and Technology, Peking University, Beijing, China

Y. Ban, G. Chen, A. Levin, J. Li, L. Li, Q. Li, Y. Mao, S.J. Qian, D. Wang, Z. Xu

Tsinghua University, Beijing, China

Y. Wang

Universidad de Los Andes, Bogota, Colombia

C. Avila, A. Cabrera, C.A. Carrillo Montoya, L.F. Chaparro Sierra, C. Florez, C.F. González Hernández, M.A. Segura Delgado

University of Split, Faculty of Electrical Engineering, Mechanical Engineering and Naval Architecture, Split, Croatia

B. Courbon, N. Godinovic, D. Lelas, I. Puljak, T. Sculac

University of Split, Faculty of Science, Split, Croatia

Z. Antunovic, M. Kovac

Institute Rudjer Boskovic, Zagreb, Croatia

V. Brigljevic, D. Ferencek, K. Kadija, B. Mesic, A. Starodumov[7], T. Susa

University of Cyprus, Nicosia, Cyprus

M.W. Ather, A. Attikis, M. Kolosova, G. Mavromanolakis, J. Mousa, C. Nicolaou, F. Ptochos, P.A. Razis, H. Rykaczewski

Charles University, Prague, Czech Republic

M. Finger[8], M. Finger Jr.[8]

JHEP11(2018)042

Escuela Politecnica Nacional, Quito, Ecuador

E. Ayala

Universidad San Francisco de Quito, Quito, Ecuador

E. Carrera Jarrin

Academy of Scientific Research and Technology of the Arab Republic of Egypt, Egyptian Network of High Energy Physics, Cairo, Egypt

Y. Assran[9,10], S. Elgammal[10], S. Khalil[11]

National Institute of Chemical Physics and Biophysics, Tallinn, Estonia

S. Bhowmik, A. Carvalho Antunes De Oliveira, R.K. Dewanjee, K. Ehataht, M. Kadastik, M. Raidal, C. Veelken

Department of Physics, University of Helsinki, Helsinki, Finland

P. Eerola, H. Kirschenmann, J. Pekkanen, M. Voutilainen

Helsinki Institute of Physics, Helsinki, Finland

J. Havukainen, J.K. Heikkilä, T. Järvinen, V. Karimäki, R. Kinnunen, T. Lampén, K. Lassila-Perini, S. Laurila, S. Lehti, T. Lindén, P. Luukka, T. Mäenpää, H. Siikonen, E. Tuominen, J. Tuominiemi

Lappeenranta University of Technology, Lappeenranta, Finland

T. Tuuva

IRFU, CEA, Université Paris-Saclay, Gif-sur-Yvette, France

M. Besancon, F. Couderc, M. Dejardin, D. Denegri, J.L. Faure, F. Ferri, S. Ganjour, A. Givernaud, P. Gras, G. Hamel de Monchenault, P. Jarry, C. Leloup, E. Locci, J. Malcles, G. Negro, J. Rander, A. Rosowsky, M.Ö. Sahin, M. Titov

Laboratoire Leprince-Ringuet, Ecole polytechnique, CNRS/IN2P3, Université Paris-Saclay, Palaiseau, France

A. Abdulsalam[12], C. Amendola, I. Antropov, F. Beaudette, P. Busson, C. Charlot, R. Granier de Cassagnac, I. Kucher, S. Lisniak, A. Lobanov, J. Martin Blanco, M. Nguyen, C. Ochando, G. Ortona, P. Pigard, R. Salerno, J.B. Sauvan, Y. Sirois, A.G. Stahl Leiton, A. Zabi, A. Zghiche

Université de Strasbourg, CNRS, IPHC UMR 7178, F-67000 Strasbourg, France

J.-L. Agram[13], J. Andrea, D. Bloch, J.-M. Brom, E.C. Chabert, V. Cherepanov, C. Collard, E. Conte[13], J.-C. Fontaine[13], D. Gelé, U. Goerlach, M. Jansová, A.-C. Le Bihan, N. Tonon, P. Van Hove

Centre de Calcul de l'Institut National de Physique Nucleaire et de Physique des Particules, CNRS/IN2P3, Villeurbanne, France

S. Gadrat

JHEP11(2018)042

Université de Lyon, Université Claude Bernard Lyon 1, CNRS-IN2P3, Institut de Physique Nucléaire de Lyon, Villeurbanne, France

S. Beauceron, C. Bernet, G. Boudoul, N. Chanon, R. Chierici, D. Contardo, P. Depasse, H. El Mamouni, J. Fay, L. Finco, S. Gascon, M. Gouzevitch, G. Grenier, B. Ille, F. Lagarde, I.B. Laktineh, H. Lattaud, M. Lethuillier, L. Mirabito, A.L. Pequegnot, S. Perries, A. Popov[14], V. Sordini, M. Vander Donckt, S. Viret, S. Zhang

Georgian Technical University, Tbilisi, Georgia

A. Khvedelidze[8]

Tbilisi State University, Tbilisi, Georgia

Z. Tsamalaidze[8]

RWTH Aachen University, I. Physikalisches Institut, Aachen, Germany

C. Autermann, L. Feld, M.K. Kiesel, K. Klein, M. Lipinski, M. Preuten, M.P. Rauch, C. Schomakers, J. Schulz, M. Teroerde, B. Wittmer, V. Zhukov[14]

RWTH Aachen University, III. Physikalisches Institut A, Aachen, Germany

A. Albert, D. Duchardt, M. Endres, M. Erdmann, T. Esch, R. Fischer, S. Ghosh, A. Güth, T. Hebbeker, C. Heidemann, K. Hoepfner, H. Keller, S. Knutzen, L. Mastrolorenzo, M. Merschmeyer, A. Meyer, P. Millet, S. Mukherjee, T. Pook, M. Radziej, H. Reithler, M. Rieger, F. Scheuch, A. Schmidt, D. Teyssier

RWTH Aachen University, III. Physikalisches Institut B, Aachen, Germany

G. Flügge, O. Hlushchenko, B. Kargoll, T. Kress, A. Künsken, T. Müller, A. Nehrkorn, A. Nowack, C. Pistone, O. Pooth, H. Sert, A. Stahl[15]

Deutsches Elektronen-Synchrotron, Hamburg, Germany

M. Aldaya Martin, T. Arndt, C. Asawatangtrakuldee, I. Babounikau, K. Beernaert, O. Behnke, U. Behrens, A. Bermúdez Martínez, D. Bertsche, A.A. Bin Anuar, K. Borras[16], V. Botta, A. Campbell, P. Connor, C. Contreras-Campana, F. Costanza, V. Danilov, A. De Wit, M.M. Defranchis, C. Diez Pardos, D. Domínguez Damiani, G. Eckerlin, T. Eichhorn, A. Elwood, E. Eren, E. Gallo[17], A. Geiser, J.M. Grados Luyando, A. Grohsjean, P. Gunnellini, M. Guthoff, M. Haranko, A. Harb, J. Hauk, H. Jung, M. Kasemann, J. Keaveney, C. Kleinwort, J. Knolle, D. Krücker, W. Lange, A. Lelek, T. Lenz, K. Lipka, W. Lohmann[18], R. Mankel, I.-A. Melzer-Pellmann, A.B. Meyer, M. Meyer, M. Missiroli, G. Mittag, J. Mnich, V. Myronenko, S.K. Pflitsch, D. Pitzl, A. Raspereza, M. Savitskyi, P. Saxena, P. Schütze, C. Schwanenberger, R. Shevchenko, A. Singh, N. Stefaniuk, H. Tholen, O. Turkot, A. Vagnerini, G.P. Van Onsem, R. Walsh, Y. Wen, K. Wichmann, C. Wissing, O. Zenaiev

University of Hamburg, Hamburg, Germany

R. Aggleton, S. Bein, L. Benato, A. Benecke, V. Blobel, M. Centis Vignali, T. Dreyer, E. Garutti, D. Gonzalez, J. Haller, A. Hinzmann, A. Karavdina, G. Kasieczka, R. Klanner, R. Kogler, N. Kovalchuk, S. Kurz, V. Kutzner, J. Lange, D. Marconi, J. Multhaup, M. Niedziela, D. Nowatschin, A. Perieanu, A. Reimers, O. Rieger, C. Scharf, P. Schleper,

JHEP11(2018)042

S. Schumann, J. Schwandt, J. Sonneveld, H. Stadie, G. Steinbrück, F.M. Stober, M. Stöver, D. Troendle, A. Vanhoefer, B. Vormwald

Institut für Experimentelle Teilchenphysik, Karlsruhe, Germany

M. Akbiyik, C. Barth, M. Baselga, S. Baur, E. Butz, R. Caspart, T. Chwalek, F. Colombo, W. De Boer, A. Dierlamm, N. Faltermann, B. Freund, M. Giffels, M.A. Harrendorf, F. Hartmann[15], S.M. Heindl, U. Husemann, F. Kassel[15], I. Katkov[14], S. Kudella, H. Mildner, S. Mitra, M.U. Mozer, Th. Müller, M. Plagge, G. Quast, K. Rabbertz, M. Schröder, I. Shvetsov, G. Sieber, H.J. Simonis, R. Ulrich, S. Wayand, M. Weber, T. Weiler, S. Williamson, C. Wöhrmann, R. Wolf

Institute of Nuclear and Particle Physics (INPP), NCSR Demokritos, Aghia Paraskevi, Greece

G. Anagnostou, G. Daskalakis, T. Geralis, A. Kyriakis, D. Loukas, G. Paspalaki, I. Topsis-Giotis

National and Kapodistrian University of Athens, Athens, Greece

G. Karathanasis, S. Kesisoglou, P. Kontaxakis, A. Panagiotou, N. Saoulidou, E. Tziaferi, K. Vellidis

National Technical University of Athens, Athens, Greece

K. Kousouris, I. Papakrivopoulos, G. Tsipolitis

University of Ioánnina, Ioánnina, Greece

I. Evangelou, C. Foudas, P. Gianneios, P. Katsoulis, P. Kokkas, S. Mallios, N. Manthos, I. Papadopoulos, E. Paradas, J. Strologas, F.A. Triantis, D. Tsitsonis

MTA-ELTE Lendület CMS Particle and Nuclear Physics Group, Eötvös Loránd University, Budapest, Hungary

M. Bartók[19], M. Csanad, N. Filipovic, P. Major, M.I. Nagy, G. Pasztor, O. Surányi, G.I. Veres

Wigner Research Centre for Physics, Budapest, Hungary

G. Bencze, C. Hajdu, D. Horvath[20], Á. Hunyadi, F. Sikler, T.Á. Vámi, V. Veszpremi, G. Vesztergombi[†]

Institute of Nuclear Research ATOMKI, Debrecen, Hungary

N. Beni, S. Czellar, J. Karancsi[21], A. Makovec, J. Molnar, Z. Szillasi

Institute of Physics, University of Debrecen, Debrecen, Hungary

P. Raics, Z.L. Trocsanyi, B. Ujvari

Indian Institute of Science (IISc), Bangalore, India

S. Choudhury, J.R. Komaragiri, P.C. Tiwari

National Institute of Science Education and Research, HBNI, Bhubaneswar, India

S. Bahinipati[22], C. Kar, P. Mal, K. Mandal, A. Nayak[23], D.K. Sahoo[22], S.K. Swain

JHEP11(2018)042

Panjab University, Chandigarh, India
S. Bansal, S.B. Beri, V. Bhatnagar, S. Chauhan, R. Chawla, N. Dhingra, R. Gupta, A. Kaur, A. Kaur, M. Kaur, S. Kaur, R. Kumar, P. Kumari, M. Lohan, A. Mehta, K. Sandeep, S. Sharma, J.B. Singh, G. Walia

University of Delhi, Delhi, India
A. Bhardwaj, B.C. Choudhary, R.B. Garg, M. Gola, S. Keshri, Ashok Kumar, S. Malhotra, M. Naimuddin, P. Priyanka, K. Ranjan, Aashaq Shah, R. Sharma

Saha Institute of Nuclear Physics, HBNI, Kolkata, India
R. Bhardwaj[24], M. Bharti, R. Bhattacharya, S. Bhattacharya, U. Bhawandeep[24], D. Bhowmik, S. Dey, S. Dutt[24], S. Dutta, S. Ghosh, K. Mondal, S. Nandan, A. Purohit, P.K. Rout, A. Roy, S. Roy Chowdhury, S. Sarkar, M. Sharan, B. Singh, S. Thakur[24]

Indian Institute of Technology Madras, Madras, India
P.K. Behera

Bhabha Atomic Research Centre, Mumbai, India
R. Chudasama, D. Dutta, V. Jha, V. Kumar, P.K. Netrakanti, L.M. Pant, P. Shukla

Tata Institute of Fundamental Research-A, Mumbai, India
T. Aziz, M.A. Bhat, S. Dugad, G.B. Mohanty, N. Sur, B. Sutar, RavindraKumar Verma

Tata Institute of Fundamental Research-B, Mumbai, India
S. Banerjee, S. Bhattacharya, S. Chatterjee, P. Das, M. Guchait, Sa. Jain, S. Karmakar, S. Kumar, M. Maity[25], G. Majumder, K. Mazumdar, N. Sahoo, T. Sarkar[25]

Indian Institute of Science Education and Research (IISER), Pune, India
S. Chauhan, S. Dube, V. Hegde, A. Kapoor, K. Kothekar, S. Pandey, A. Rane, S. Sharma

Institute for Research in Fundamental Sciences (IPM), Tehran, Iran
S. Chenarani[26], E. Eskandari Tadavani, S.M. Etesami[26], M. Khakzad, M. Mohammadi Najafabadi, M. Naseri, F. Rezaei Hosseinabadi, B. Safarzadeh[27], M. Zeinali

University College Dublin, Dublin, Ireland
M. Felcini, M. Grunewald

INFN Sezione di Bari [a], Università di Bari [b], Politecnico di Bari [c], Bari, Italy
M. Abbrescia[a,b], C. Calabria[a,b], A. Colaleo[a], D. Creanza[a,c], L. Cristella[a,b], N. De Filippis[a,c], M. De Palma[a,b], A. Di Florio[a,b], F. Errico[a,b], L. Fiore[a], A. Gelmi[a,b], G. Iaselli[a,c], M. Ince[a,b], S. Lezki[a,b], G. Maggi[a,c], M. Maggi[a], G. Miniello[a,b], S. My[a,b], S. Nuzzo[a,b], A. Pompili[a,b], G. Pugliese[a,c], R. Radogna[a], A. Ranieri[a], G. Selvaggi[a,b], A. Sharma[a], L. Silvestris[a], R. Venditti[a], P. Verwilligen[a], G. Zito[a]

INFN Sezione di Bologna [a], Università di Bologna [b], Bologna, Italy
G. Abbiendi[a], C. Battilana[a,b], D. Bonacorsi[a,b], L. Borgonovi[a,b], S. Braibant-Giacomelli[a,b], R. Campanini[a,b], P. Capiluppi[a,b], A. Castro[a,b], F.R. Cavallo[a], S.S. Chhibra[a,b], C. Ciocca[a], G. Codispoti[a,b], M. Cuffiani[a,b], G.M. Dallavalle[a], F. Fabbri[a], A. Fanfani[a,b], P. Giacomelli[a], C. Grandi[a], L. Guiducci[a,b], F. Iemmi[a,b], S. Marcellini[a], G. Masetti[a], A. Montanari[a],

JHEP11(2018)042

F.L. Navarria[a,b], A. Perrotta[a], F. Primavera[a,b,15], A.M. Rossi[a,b], T. Rovelli[a,b], G.P. Siroli[a,b], N. Tosi[a]

INFN Sezione di Catania [a], Università di Catania [b], Catania, Italy

S. Albergo[a,b], A. Di Mattia[a], R. Potenza[a,b], A. Tricomi[a,b], C. Tuve[a,b]

INFN Sezione di Firenze [a], Università di Firenze [b], Firenze, Italy

G. Barbagli[a], K. Chatterjee[a,b], V. Ciulli[a,b], C. Civinini[a], R. D'Alessandro[a,b], E. Focardi[a,b], G. Latino, P. Lenzi[a,b], M. Meschini[a], S. Paoletti[a], L. Russo[a,28], G. Sguazzoni[a], D. Strom[a], L. Viliani[a]

INFN Laboratori Nazionali di Frascati, Frascati, Italy

L. Benussi, S. Bianco, F. Fabbri, D. Piccolo

INFN Sezione di Genova [a], Università di Genova [b], Genova, Italy

F. Ferro[a], F. Ravera[a,b], E. Robutti[a], S. Tosi[a,b]

INFN Sezione di Milano-Bicocca [a], Università di Milano-Bicocca [b], Milano, Italy

A. Benaglia[a], A. Beschi[b], L. Brianza[a,b], F. Brivio[a,b], V. Ciriolo[a,b,15], S. Di Guida[a,d,15], M.E. Dinardo[a,b], S. Fiorendi[a,b], S. Gennai[a], A. Ghezzi[a,b], P. Govoni[a,b], M. Malberti[a,b], S. Malvezzi[a], A. Massironi[a,b], D. Menasce[a], L. Moroni[a], M. Paganoni[a,b], D. Pedrini[a], S. Ragazzi[a,b], T. Tabarelli de Fatis[a,b]

INFN Sezione di Napoli [a], Università di Napoli 'Federico II' [b], Napoli, Italy, Università della Basilicata [c], Potenza, Italy, Università G. Marconi [d], Roma, Italy

S. Buontempo[a], N. Cavallo[a,c], A. Di Crescenzo[a,b], F. Fabozzi[a,c], F. Fienga[a], G. Galati[a], A.O.M. Iorio[a,b], W.A. Khan[a], L. Lista[a], S. Meola[a,d,15], P. Paolucci[a,15], C. Sciacca[a,b], E. Voevodina[a,b]

INFN Sezione di Padova [a], Università di Padova [b], Padova, Italy, Università di Trento [c], Trento, Italy

P. Azzi[a], N. Bacchetta[a], D. Bisello[a,b], A. Boletti[a,b], A. Bragagnolo, M. Dall'Osso[a,b], P. De Castro Manzano[a], T. Dorigo[a], U. Dosselli[a], F. Gasparini[a,b], U. Gasparini[a,b], A. Gozzelino[a], S. Lacaprara[a], P. Lujan, M. Margoni[a,b], A.T. Meneguzzo[a,b], F. Montecassiano[a], J. Pazzini[a,b], N. Pozzobon[a,b], P. Ronchese[a,b], R. Rossin[a,b], F. Simonetto[a,b], A. Tiko, E. Torassa[a], M. Zanetti[a,b], P. Zotto[a,b], G. Zumerle[a,b]

INFN Sezione di Pavia [a], Università di Pavia [b], Pavia, Italy

A. Braghieri[a], A. Magnani[a], P. Montagna[a,b], S.P. Ratti[a,b], V. Re[a], M. Ressegotti[a,b], C. Riccardi[a,b], P. Salvini[a], I. Vai[a,b], P. Vitulo[a,b]

INFN Sezione di Perugia [a], Università di Perugia [b], Perugia, Italy

L. Alunni Solestizi[a,b], M. Biasini[a,b], G.M. Bilei[a], C. Cecchi[a,b], D. Ciangottini[a,b], L. Fanò[a,b], P. Lariccia[a,b], R. Leonardi[a,b], E. Manoni[a], G. Mantovani[a,b], V. Mariani[a,b], M. Menichelli[a], A. Rossi[a,b], A. Santocchia[a,b], D. Spiga[a]

JHEP11(2018)042

INFN Sezione di Pisa [a], Università di Pisa [b], Scuola Normale Superiore di Pisa [c], Pisa, Italy

K. Androsov[a], P. Azzurri[a], G. Bagliesi[a], L. Bianchini[a], T. Boccali[a], L. Borrello, R. Castaldi[a], M.A. Ciocci[a,b], R. Dell'Orso[a], G. Fedi[a], F. Fiori[a,c], L. Giannini[a,c], A. Giassi[a], M.T. Grippo[a], F. Ligabue[a,c], E. Manca[a,c], G. Mandorli[a,c], A. Messineo[a,b], F. Palla[a], A. Rizzi[a,b], P. Spagnolo[a], R. Tenchini[a], G. Tonelli[a,b], A. Venturi[a], P.G. Verdini[a]

INFN Sezione di Roma [a], Sapienza Università di Roma [b], Rome, Italy

L. Barone[a,b], F. Cavallari[a], M. Cipriani[a,b], N. Daci[a], D. Del Re[a,b], E. Di Marco[a,b], M. Diemoz[a], S. Gelli[a,b], E. Longo[a,b], B. Marzocchi[a,b], P. Meridiani[a], G. Organtini[a,b], F. Pandolfi[a], R. Paramatti[a,b], F. Preiato[a,b], S. Rahatlou[a,b], C. Rovelli[a], F. Santanastasio[a,b]

INFN Sezione di Torino [a], Università di Torino [b], Torino, Italy, Università del Piemonte Orientale [c], Novara, Italy

N. Amapane[a,b], R. Arcidiacono[a,c], S. Argiro[a,b], M. Arneodo[a,c], N. Bartosik[a], R. Bellan[a,b], C. Biino[a], N. Cartiglia[a], F. Cenna[a,b], S. Cometti, M. Costa[a,b], R. Covarelli[a,b], N. Demaria[a], B. Kiani[a,b], C. Mariotti[a], S. Maselli[a], E. Migliore[a,b], V. Monaco[a,b], E. Monteil[a,b], M. Monteno[a], M.M. Obertino[a,b], L. Pacher[a,b], N. Pastrone[a], M. Pelliccioni[a], G.L. Pinna Angioni[a,b], A. Romero[a,b], M. Ruspa[a,c], R. Sacchi[a,b], K. Shchelina[a,b], V. Sola[a], A. Solano[a,b], D. Soldi, A. Staiano[a]

INFN Sezione di Trieste [a], Università di Trieste [b], Trieste, Italy

S. Belforte[a], V. Candelise[a,b], M. Casarsa[a], F. Cossutti[a], G. Della Ricca[a,b], F. Vazzoler[a,b], A. Zanetti[a]

Kyungpook National University

D.H. Kim, G.N. Kim, M.S. Kim, J. Lee, S. Lee, S.W. Lee, C.S. Moon, Y.D. Oh, S. Sekmen, D.C. Son, Y.C. Yang

Chonnam National University, Institute for Universe and Elementary Particles, Kwangju, Korea

H. Kim, D.H. Moon, G. Oh

Hanyang University, Seoul, Korea

J. Goh[29], T.J. Kim

Korea University, Seoul, Korea

S. Cho, S. Choi, Y. Go, D. Gyun, S. Ha, B. Hong, Y. Jo, K. Lee, K.S. Lee, S. Lee, J. Lim, S.K. Park, Y. Roh

Sejong University, Seoul, Korea

H.S. Kim

Seoul National University, Seoul, Korea

J. Almond, J. Kim, J.S. Kim, H. Lee, K. Lee, K. Nam, S.B. Oh, B.C. Radburn-Smith, S.h. Seo, U.K. Yang, H.D. Yoo, G.B. Yu

University of Seoul, Seoul, Korea

D. Jeon, H. Kim, J.H. Kim, J.S.H. Lee, I.C. Park

JHEP11(2018)042

Sungkyunkwan University, Suwon, Korea

Y. Choi, C. Hwang, J. Lee, I. Yu

Vilnius University, Vilnius, Lithuania

V. Dudenas, A. Juodagalvis, J. Vaitkus

National Centre for Particle Physics, Universiti Malaya, Kuala Lumpur, Malaysia

I. Ahmed, Z.A. Ibrahim, M.A.B. Md Ali[30], F. Mohamad Idris[31], W.A.T. Wan Abdullah, M.N. Yusli, Z. Zolkapli

Universidad de Sonora (UNISON), Hermosillo, Mexico

A. Castaneda Hernandez, J.A. Murillo Quijada

Centro de Investigacion y de Estudios Avanzados del IPN, Mexico City, Mexico

M.C. Duran-Osuna, H. Castilla-Valdez, E. De La Cruz-Burelo, G. Ramirez-Sanchez, I. Heredia-De La Cruz[32], R.I. Rabadan-Trejo, R. Lopez-Fernandez, J. Mejia Guisao, R Reyes-Almanza, A. Sanchez-Hernandez

Universidad Iberoamericana, Mexico City, Mexico

S. Carrillo Moreno, C. Oropeza Barrera, F. Vazquez Valencia

Benemerita Universidad Autonoma de Puebla, Puebla, Mexico

J. Eysermans, I. Pedraza, H.A. Salazar Ibarguen, C. Uribe Estrada

Universidad Autónoma de San Luis Potosí, San Luis Potosí, Mexico

A. Morelos Pineda

University of Auckland, Auckland, New Zealand

D. Krofcheck

University of Canterbury, Christchurch, New Zealand

S. Bheesette, P.H. Butler

National Centre for Physics, Quaid-I-Azam University, Islamabad, Pakistan

A. Ahmad, M. Ahmad, M.I. Asghar, Q. Hassan, H.R. Hoorani, A. Saddique, M.A. Shah, M. Shoaib, M. Waqas

National Centre for Nuclear Research, Swierk, Poland

H. Bialkowska, M. Bluj, B. Boimska, T. Frueboes, M. Górski, M. Kazana, K. Nawrocki, M. Szleper, P. Traczyk, P. Zalewski

Institute of Experimental Physics, Faculty of Physics, University of Warsaw, Warsaw, Poland

K. Bunkowski, A. Byszuk[33], K. Doroba, A. Kalinowski, M. Konecki, J. Krolikowski, M. Misiura, M. Olszewski, A. Pyskir, M. Walczak

JHEP11(2018)042

Laboratório de Instrumentação e Física Experimental de Partículas, Lisboa, Portugal

P. Bargassa, C. Beirão Da Cruz E Silva, A. Di Francesco, P. Faccioli, B. Galinhas, M. Gallinaro, J. Hollar, N. Leonardo, L. Lloret Iglesias, M.V. Nemallapudi, J. Seixas, G. Strong, O. Toldaiev, D. Vadruccio, J. Varela

Joint Institute for Nuclear Research, Dubna, Russia

S. Afanasiev, V. Alexakhin, P. Bunin, M. Gavrilenko, A. Golunov, I. Golutvin, N. Gorbounov, V. Karjavin, A. Lanev, A. Malakhov, V. Matveev[34,35], P. Moisenz, V. Palichik, V. Perelygin, M. Savina, S. Shmatov, V. Smirnov, N. Voytishin, A. Zarubin

Petersburg Nuclear Physics Institute, Gatchina (St. Petersburg), Russia

V. Golovtsov, Y. Ivanov, V. Kim[36], E. Kuznetsova[37], P. Levchenko, V. Murzin, V. Oreshkin, I. Smirnov, D. Sosnov, V. Sulimov, L. Uvarov, S. Vavilov, A. Vorobyev

Institute for Nuclear Research, Moscow, Russia

Yu. Andreev, A. Dermenev, S. Gninenko, N. Golubev, A. Karneyeu, M. Kirsanov, N. Krasnikov, A. Pashenkov, D. Tlisov, A. Toropin

Institute for Theoretical and Experimental Physics, Moscow, Russia

V. Epshteyn, V. Gavrilov, N. Lychkovskaya, V. Popov, I. Pozdnyakov, G. Safronov, A. Spiridonov, A. Stepennov, V. Stolin, M. Toms, E. Vlasov, A. Zhokin

Moscow Institute of Physics and Technology, Moscow, Russia

T. Aushev

National Research Nuclear University 'Moscow Engineering Physics Institute' (MEPhI), Moscow, Russia

R. Chistov[38], M. Danilov[38], P. Parygin, D. Philippov, S. Polikarpov[38], E. Tarkovskii

P.N. Lebedev Physical Institute, Moscow, Russia

V. Andreev, M. Azarkin[35], I. Dremin[35], M. Kirakosyan[35], S.V. Rusakov, A. Terkulov

Skobeltsyn Institute of Nuclear Physics, Lomonosov Moscow State University, Moscow, Russia

A. Baskakov, A. Belyaev, E. Boos, M. Dubinin[39], L. Dudko, A. Ershov, A. Gribushin, V. Klyukhin, O. Kodolova, I. Lokhtin, I. Miagkov, S. Obraztsov, S. Petrushanko, V. Savrin, A. Snigirev

Novosibirsk State University (NSU), Novosibirsk, Russia

V. Blinov[40], T. Dimova[40], L. Kardapoltsev[40], D. Shtol[40], Y. Skovpen[40]

State Research Center of Russian Federation, Institute for High Energy Physics of NRC 'Kurchatov Institute', Protvino, Russia

I. Azhgirey, I. Bayshev, S. Bitioukov, D. Elumakhov, A. Godizov, V. Kachanov, A. Kalinin, D. Konstantinov, P. Mandrik, V. Petrov, R. Ryutin, S. Slabospitskii, A. Sobol, S. Troshin, N. Tyurin, A. Uzunian, A. Volkov

JHEP11(2018)042

National Research Tomsk Polytechnic University, Tomsk, Russia

A. Babaev, S. Baidali

University of Belgrade, Faculty of Physics and Vinca Institute of Nuclear Sciences, Belgrade, Serbia

P. Adzic[41], P. Cirkovic, D. Devetak, M. Dordevic, J. Milosevic

Centro de Investigaciones Energéticas Medioambientales y Tecnológicas (CIEMAT), Madrid, Spain

J. Alcaraz Maestre, A. Álvarez Fernández, I. Bachiller, M. Barrio Luna, J.A. Brochero Cifuentes, M. Cerrada, N. Colino, B. De La Cruz, A. Delgado Peris, C. Fernandez Bedoya, J.P. Fernández Ramos, J. Flix, M.C. Fouz, O. Gonzalez Lopez, S. Goy Lopez, J.M. Hernandez, M.I. Josa, D. Moran, A. Pérez-Calero Yzquierdo, J. Puerta Pelayo, I. Redondo, L. Romero, M.S. Soares, A. Triossi

Universidad Autónoma de Madrid, Madrid, Spain

C. Albajar, J.F. de Trocóniz

Universidad de Oviedo, Oviedo, Spain

J. Cuevas, C. Erice, J. Fernandez Menendez, S. Folgueras, I. Gonzalez Caballero, J.R. González Fernández, E. Palencia Cortezon, V. Rodríguez Bouza, S. Sanchez Cruz, P. Vischia, J.M. Vizan Garcia

Instituto de Física de Cantabria (IFCA), CSIC-Universidad de Cantabria, Santander, Spain

I.J. Cabrillo, A. Calderon, B. Chazin Quero, J. Duarte Campderros, M. Fernandez, P.J. Fernández Manteca, A. García Alonso, J. Garcia-Ferrero, G. Gomez, A. Lopez Virto, J. Marco, C. Martinez Rivero, P. Martinez Ruiz del Arbol, F. Matorras, J. Piedra Gomez, C. Prieels, T. Rodrigo, A. Ruiz-Jimeno, L. Scodellaro, N. Trevisani, I. Vila, R. Vilar Cortabitarte

CERN, European Organization for Nuclear Research, Geneva, Switzerland

D. Abbaneo, B. Akgun, E. Auffray, P. Baillon, A.H. Ball, D. Barney, J. Bendavid, M. Bianco, A. Bocci, C. Botta, E. Brondolin, T. Camporesi, M. Cepeda, G. Cerminara, E. Chapon, Y. Chen, G. Cucciati, D. d'Enterria, A. Dabrowski, V. Daponte, A. David, A. De Roeck, N. Deelen, M. Dobson, T. du Pree, M. Dünser, N. Dupont, A. Elliott-Peisert, P. Everaerts, F. Fallavollita[42], D. Fasanella, G. Franzoni, J. Fulcher, W. Funk, D. Gigi, A. Gilbert, K. Gill, F. Glege, M. Guilbaud, D. Gulhan, J. Hegeman, V. Innocente, A. Jafari, P. Janot, O. Karacheban[18], J. Kieseler, A. Kornmayer, M. Krammer[1], C. Lange, P. Lecoq, C. Lourenço, L. Malgeri, M. Mannelli, F. Meijers, J.A. Merlin, S. Mersi, E. Meschi, P. Milenovic[43], F. Moortgat, M. Mulders, J. Ngadiuba, S. Orfanelli, L. Orsini, F. Pantaleo[15], L. Pape, E. Perez, M. Peruzzi, A. Petrilli, G. Petrucciani, A. Pfeiffer, M. Pierini, F.M. Pitters, D. Rabady, A. Racz, T. Reis, G. Rolandi[44], M. Rovere, H. Sakulin, C. Schäfer, C. Schwick, M. Seidel, M. Selvaggi, A. Sharma, P. Silva, P. Sphicas[45], A. Stakia, J. Steggemann, M. Tosi, D. Treille, A. Tsirou, V. Veckalns[46], W.D. Zeuner

JHEP11(2018)042

Paul Scherrer Institut, Villigen, Switzerland

L. Caminada[47], K. Deiters, W. Erdmann, R. Horisberger, Q. Ingram, H.C. Kaestli, D. Kotlinski, U. Langenegger, T. Rohe, S.A. Wiederkehr

ETH Zurich — Institute for Particle Physics and Astrophysics (IPA), Zurich, Switzerland

M. Backhaus, L. Bäni, P. Berger, N. Chernyavskaya, G. Dissertori, M. Dittmar, M. Donegà, C. Dorfer, C. Grab, C. Heidegger, D. Hits, J. Hoss, T. Klijnsma, W. Lustermann, R.A. Manzoni, M. Marionneau, M.T. Meinhard, F. Micheli, P. Musella, F. Nessi-Tedaldi, J. Pata, F. Pauss, G. Perrin, L. Perrozzi, S. Pigazzini, M. Quittnat, D. Ruini, D.A. Sanz Becerra, M. Schönenberger, L. Shchutska, V.R. Tavolaro, K. Theofilatos, M.L. Vesterbacka Olsson, R. Wallny, D.H. Zhu

Universität Zürich, Zurich, Switzerland

T.K. Aarrestad, C. Amsler[48], D. Brzhechko, M.F. Canelli, A. De Cosa, R. Del Burgo, S. Donato, C. Galloni, T. Hreus, B. Kilminster, I. Neutelings, D. Pinna, G. Rauco, P. Robmann, D. Salerno, K. Schweiger, C. Seitz, Y. Takahashi, A. Zucchetta

National Central University, Chung-Li, Taiwan

Y.H. Chang, K.y. Cheng, T.H. Doan, Sh. Jain, R. Khurana, C.M. Kuo, W. Lin, A. Pozdnyakov, S.S. Yu

National Taiwan University (NTU), Taipei, Taiwan

P. Chang, Y. Chao, K.F. Chen, P.H. Chen, W.-S. Hou, Arun Kumar, Y.y. Li, Y.F. Liu, R.-S. Lu, E. Paganis, A. Psallidas, A. Steen, J.f. Tsai

Chulalongkorn University, Faculty of Science, Department of Physics, Bangkok, Thailand

B. Asavapibhop, N. Srimanobhas, N. Suwonjandee

Çukurova University, Physics Department, Science and Art Faculty, Adana, Turkey

A. Bat, F. Boran, S. Cerci[49], S. Damarseckin, Z.S. Demiroglu, F. Dolek, C. Dozen, I. Dumanoglu, S. Girgis, G. Gokbulut, Y. Guler, E. Gurpinar, I. Hos[50], C. Isik, E.E. Kangal[51], O. Kara, A. Kayis Topaksu, U. Kiminsu, M. Oglakci, G. Onengut, K. Ozdemir[52], S. Ozturk[53], D. Sunar Cerci[49], B. Tali[49], U.G. Tok, S. Turkcapar, I.S. Zorbakir, C. Zorbilmez

Middle East Technical University, Physics Department, Ankara, Turkey

B. Isildak[54], G. Karapinar[55], M. Yalvac, M. Zeyrek

Bogazici University, Istanbul, Turkey

I.O. Atakisi, E. Gülmez, M. Kaya[56], O. Kaya[57], S. Tekten, E.A. Yetkin[58]

Istanbul Technical University, Istanbul, Turkey

M.N. Agaras, S. Atay, A. Cakir, K. Cankocak, Y. Komurcu, S. Sen[59]

JHEP11(2018)042

Institute for Scintillation Materials of National Academy of Science of Ukraine, Kharkov, Ukraine

B. Grynyov

National Scientific Center, Kharkov Institute of Physics and Technology, Kharkov, Ukraine

L. Levchuk

University of Bristol, Bristol, United Kingdom

F. Ball, L. Beck, J.J. Brooke, D. Burns, E. Clement, D. Cussans, O. Davignon, H. Flacher, J. Goldstein, G.P. Heath, H.F. Heath, L. Kreczko, D.M. Newbold[60], S. Paramesvaran, B. Penning, T. Sakuma, D. Smith, V.J. Smith, J. Taylor, A. Titterton

Rutherford Appleton Laboratory, Didcot, United Kingdom

K.W. Bell, A. Belyaev[61], C. Brew, R.M. Brown, D. Cieri, D.J.A. Cockerill, J.A. Coughlan, K. Harder, S. Harper, J. Linacre, E. Olaiya, D. Petyt, C.H. Shepherd-Themistocleous, A. Thea, I.R. Tomalin, T. Williams, W.J. Womersley

Imperial College, London, United Kingdom

G. Auzinger, R. Bainbridge, P. Bloch, J. Borg, S. Breeze, O. Buchmuller, A. Bundock, S. Casasso, D. Colling, L. Corpe, P. Dauncey, G. Davies, M. Della Negra, R. Di Maria, Y. Haddad, G. Hall, G. Iles, T. James, M. Komm, C. Laner, L. Lyons, A.-M. Magnan, S. Malik, A. Martelli, J. Nash[62], A. Nikitenko[7], V. Palladino, M. Pesaresi, A. Richards, A. Rose, E. Scott, C. Seez, A. Shtipliyski, G. Singh, M. Stoye, T. Strebler, S. Summers, A. Tapper, K. Uchida, T. Virdee[15], N. Wardle, D. Winterbottom, J. Wright, S.C. Zenz

Brunel University, Uxbridge, United Kingdom

J.E. Cole, P.R. Hobson, A. Khan, P. Kyberd, C.K. Mackay, A. Morton, I.D. Reid, L. Teodorescu, S. Zahid

Baylor University, Waco, U.S.A.

K. Call, J. Dittmann, K. Hatakeyama, H. Liu, C. Madrid, B. Mcmaster, N. Pastika, C. Smith

Catholic University of America, Washington DC, U.S.A.

R. Bartek, A. Dominguez

The University of Alabama, Tuscaloosa, U.S.A.

A. Buccilli, S.I. Cooper, C. Henderson, P. Rumerio, C. West

Boston University, Boston, U.S.A.

D. Arcaro, T. Bose, D. Gastler, D. Rankin, C. Richardson, J. Rohlf, L. Sulak, D. Zou

Brown University, Providence, U.S.A.

G. Benelli, X. Coubez, D. Cutts, M. Hadley, J. Hakala, U. Heintz, J.M. Hogan[63], K.H.M. Kwok, E. Laird, G. Landsberg, J. Lee, Z. Mao, M. Narain, S. Piperov, S. Sagir[64], R. Syarif, E. Usai, D. Yu

JHEP11(2018)042

University of California, Davis, Davis, U.S.A.

R. Band, C. Brainerd, R. Breedon, D. Burns, M. Calderon De La Barca Sanchez, M. Chertok, J. Conway, R. Conway, P.T. Cox, R. Erbacher, C. Flores, G. Funk, W. Ko, O. Kukral, R. Lander, C. Mclean, M. Mulhearn, D. Pellett, J. Pilot, S. Shalhout, M. Shi, D. Stolp, D. Taylor, K. Tos, M. Tripathi, Z. Wang, F. Zhang

University of California, Los Angeles, U.S.A.

M. Bachtis, C. Bravo, R. Cousins, A. Dasgupta, A. Florent, J. Hauser, M. Ignatenko, N. Mccoll, S. Regnard, D. Saltzberg, C. Schnaible, V. Valuev

University of California, Riverside, Riverside, U.S.A.

E. Bouvier, K. Burt, R. Clare, J.W. Gary, S.M.A. Ghiasi Shirazi, G. Hanson, G. Karapostoli, E. Kennedy, F. Lacroix, O.R. Long, M. Olmedo Negrete, M.I. Paneva, W. Si, L. Wang, H. Wei, S. Wimpenny, B.R. Yates

University of California, San Diego, La Jolla, U.S.A.

J.G. Branson, S. Cittolin, M. Derdzinski, R. Gerosa, D. Gilbert, B. Hashemi, A. Holzner, D. Klein, G. Kole, V. Krutelyov, J. Letts, M. Masciovecchio, D. Olivito, S. Padhi, M. Pieri, M. Sani, V. Sharma, S. Simon, M. Tadel, A. Vartak, S. Wasserbaech[65], J. Wood, F. Würthwein, A. Yagil, G. Zevi Della Porta

University of California, Santa Barbara — Department of Physics, Santa Barbara, U.S.A.

N. Amin, R. Bhandari, J. Bradmiller-Feld, C. Campagnari, M. Citron, A. Dishaw, V. Dutta, M. Franco Sevilla, L. Gouskos, R. Heller, J. Incandela, A. Ovcharova, H. Qu, J. Richman, D. Stuart, I. Suarez, S. Wang, J. Yoo

California Institute of Technology, Pasadena, U.S.A.

D. Anderson, A. Bornheim, J.M. Lawhorn, H.B. Newman, T.Q. Nguyen, M. Spiropulu, J.R. Vlimant, R. Wilkinson, S. Xie, Z. Zhang, R.Y. Zhu

Carnegie Mellon University, Pittsburgh, U.S.A.

M.B. Andrews, T. Ferguson, T. Mudholkar, M. Paulini, M. Sun, I. Vorobiev, M. Weinberg

University of Colorado Boulder, Boulder, U.S.A.

J.P. Cumalat, W.T. Ford, F. Jensen, A. Johnson, M. Krohn, S. Leontsinis, E. MacDonald, T. Mulholland, K. Stenson, K.A. Ulmer, S.R. Wagner

Cornell University, Ithaca, U.S.A.

J. Alexander, J. Chaves, Y. Cheng, J. Chu, A. Datta, K. Mcdermott, N. Mirman, J.R. Patterson, D. Quach, A. Rinkevicius, A. Ryd, L. Skinnari, L. Soffi, S.M. Tan, Z. Tao, J. Thom, J. Tucker, P. Wittich, M. Zientek

Fermi National Accelerator Laboratory, Batavia, U.S.A.

S. Abdullin, M. Albrow, M. Alyari, G. Apollinari, A. Apresyan, A. Apyan, S. Banerjee, L.A.T. Bauerdick, A. Beretvas, J. Berryhill, P.C. Bhat, G. Bolla†, K. Burkett, J.N. Butler, A. Canepa, G.B. Cerati, H.W.K. Cheung, F. Chlebana, M. Cremonesi, J. Duarte, V.D. Elvira, J. Freeman, Z. Gecse, E. Gottschalk, L. Gray, D. Green, S. Grünendahl,

JHEP11(2018)042

O. Gutsche, J. Hanlon, R.M. Harris, S. Hasegawa, J. Hirschauer, Z. Hu, B. Jayatilaka, S. Jindariani, M. Johnson, U. Joshi, B. Klima, M.J. Kortelainen, B. Kreis, S. Lammel, D. Lincoln, R. Lipton, M. Liu, T. Liu, J. Lykken, K. Maeshima, J.M. Marraffino, D. Mason, P. McBride, P. Merkel, S. Mrenna, S. Nahn, V. O'Dell, K. Pedro, C. Pena, O. Prokofyev, G. Rakness, L. Ristori, A. Savoy-Navarro[66], B. Schneider, E. Sexton-Kennedy, A. Soha, W.J. Spalding, L. Spiegel, S. Stoynev, J. Strait, N. Strobbe, L. Taylor, S. Tkaczyk, N.V. Tran, L. Uplegger, E.W. Vaandering, C. Vernieri, M. Verzocchi, R. Vidal, M. Wang, H.A. Weber, A. Whitbeck

University of Florida, Gainesville, U.S.A.

D. Acosta, P. Avery, P. Bortignon, D. Bourilkov, A. Brinkerhoff, L. Cadamuro, A. Carnes, M. Carver, D. Curry, R.D. Field, S.V. Gleyzer, B.M. Joshi, J. Konigsberg, A. Korytov, P. Ma, K. Matchev, H. Mei, G. Mitselmakher, K. Shi, D. Sperka, J. Wang, S. Wang

Florida International University, Miami, U.S.A.

Y.R. Joshi, S. Linn

Florida State University, Tallahassee, U.S.A.

A. Ackert, T. Adams, A. Askew, S. Hagopian, V. Hagopian, K.F. Johnson, T. Kolberg, G. Martinez, T. Perry, H. Prosper, A. Saha, V. Sharma, R. Yohay

Florida Institute of Technology, Melbourne, U.S.A.

M.M. Baarmand, V. Bhopatkar, S. Colafranceschi, M. Hohlmann, D. Noonan, M. Rahmani, T. Roy, F. Yumiceva

University of Illinois at Chicago (UIC), Chicago, U.S.A.

M.R. Adams, L. Apanasevich, D. Berry, R.R. Betts, R. Cavanaugh, X. Chen, S. Dittmer, O. Evdokimov, C.E. Gerber, D.A. Hangal, D.J. Hofman, K. Jung, J. Kamin, C. Mills, I.D. Sandoval Gonzalez, M.B. Tonjes, N. Varelas, H. Wang, X. Wang, Z. Wu, J. Zhang

The University of Iowa, Iowa City, U.S.A.

M. Alhusseini, B. Bilki[67], W. Clarida, K. Dilsiz[68], S. Durgut, R.P. Gandrajula, M. Haytmyradov, V. Khristenko, J.-P. Merlo, A. Mestvirishvili, A. Moeller, J. Nachtman, H. Ogul[69], Y. Onel, F. Ozok[70], A. Penzo, C. Snyder, E. Tiras, J. Wetzel

Johns Hopkins University, Baltimore, U.S.A.

B. Blumenfeld, A. Cocoros, N. Eminizer, D. Fehling, L. Feng, A.V. Gritsan, W.T. Hung, P. Maksimovic, J. Roskes, U. Sarica, M. Swartz, M. Xiao, C. You

The University of Kansas, Lawrence, U.S.A.

A. Al-bataineh, P. Baringer, A. Bean, S. Boren, J. Bowen, A. Bylinkin, J. Castle, S. Khalil, A. Kropivnitskaya, D. Majumder, W. Mcbrayer, M. Murray, C. Rogan, S. Sanders, E. Schmitz, J.D. Tapia Takaki, Q. Wang

Kansas State University, Manhattan, U.S.A.

S. Duric, A. Ivanov, K. Kaadze, D. Kim, Y. Maravin, D.R. Mendis, T. Mitchell, A. Modak, A. Mohammadi, L.K. Saini, N. Skhirtladze

JHEP11(2018)042

Lawrence Livermore National Laboratory, Livermore, U.S.A.

F. Rebassoo, D. Wright

University of Maryland, College Park, U.S.A.

A. Baden, O. Baron, A. Belloni, S.C. Eno, Y. Feng, C. Ferraioli, N.J. Hadley, S. Jabeen, G.Y. Jeng, R.G. Kellogg, J. Kunkle, A.C. Mignerey, F. Ricci-Tam, Y.H. Shin, A. Skuja, S.C. Tonwar, K. Wong

Massachusetts Institute of Technology, Cambridge, U.S.A.

D. Abercrombie, B. Allen, V. Azzolini, A. Baty, G. Bauer, R. Bi, S. Brandt, W. Busza, I.A. Cali, M. D'Alfonso, Z. Demiragli, G. Gomez Ceballos, M. Goncharov, P. Harris, D. Hsu, M. Hu, Y. Iiyama, G.M. Innocenti, M. Klute, D. Kovalskyi, Y.-J. Lee, P.D. Luckey, B. Maier, A.C. Marini, C. Mcginn, C. Mironov, S. Narayanan, X. Niu, C. Paus, C. Roland, G. Roland, G.S.F. Stephans, K. Sumorok, K. Tatar, D. Velicanu, J. Wang, T.W. Wang, B. Wyslouch, S. Zhaozhong

University of Minnesota, Minneapolis, U.S.A.

A.C. Benvenuti, R.M. Chatterjee, A. Evans, P. Hansen, S. Kalafut, Y. Kubota, Z. Lesko, J. Mans, S. Nourbakhsh, N. Ruckstuhl, R. Rusack, J. Turkewitz, M.A. Wadud

University of Mississippi, Oxford, U.S.A.

J.G. Acosta, S. Oliveros

University of Nebraska-Lincoln, Lincoln, U.S.A.

E. Avdeeva, K. Bloom, D.R. Claes, C. Fangmeier, F. Golf, R. Gonzalez Suarez, R. Kamalieddin, I. Kravchenko, J. Monroy, J.E. Siado, G.R. Snow, B. Stieger

State University of New York at Buffalo, Buffalo, U.S.A.

A. Godshalk, C. Harrington, I. Iashvili, A. Kharchilava, D. Nguyen, A. Parker, S. Rappoccio, B. Roozbahani

Northeastern University, Boston, U.S.A.

E. Barberis, C. Freer, A. Hortiangtham, D.M. Morse, T. Orimoto, R. Teixeira De Lima, T. Wamorkar, B. Wang, A. Wisecarver, D. Wood

Northwestern University, Evanston, U.S.A.

S. Bhattacharya, O. Charaf, K.A. Hahn, N. Mucia, N. Odell, M.H. Schmitt, K. Sung, M. Trovato, M. Velasco

University of Notre Dame, Notre Dame, U.S.A.

R. Bucci, N. Dev, M. Hildreth, K. Hurtado Anampa, C. Jessop, D.J. Karmgard, N. Kellams, K. Lannon, W. Li, N. Loukas, N. Marinelli, F. Meng, C. Mueller, Y. Musienko[34], M. Planer, A. Reinsvold, R. Ruchti, P. Siddireddy, G. Smith, S. Taroni, M. Wayne, A. Wightman, M. Wolf, A. Woodard

The Ohio State University, Columbus, U.S.A.

J. Alimena, L. Antonelli, B. Bylsma, L.S. Durkin, S. Flowers, B. Francis, A. Hart, C. Hill, W. Ji, T.Y. Ling, W. Luo, B.L. Winer, H.W. Wulsin

JHEP11(2018)042

Princeton University, Princeton, U.S.A.

S. Cooperstein, P. Elmer, J. Hardenbrook, P. Hebda, S. Higginbotham, A. Kalogeropoulos, D. Lange, M.T. Lucchini, J. Luo, D. Marlow, K. Mei, I. Ojalvo, J. Olsen, C. Palmer, P. Piroué, J. Salfeld-Nebgen, D. Stickland, C. Tully

University of Puerto Rico, Mayaguez, U.S.A.

S. Malik, S. Norberg

Purdue University, West Lafayette, U.S.A.

A. Barker, V.E. Barnes, S. Das, L. Gutay, M. Jones, A.W. Jung, A. Khatiwada, B. Mahakud, D.H. Miller, N. Neumeister, C.C. Peng, H. Qiu, J.F. Schulte, J. Sun, F. Wang, R. Xiao, W. Xie

Purdue University Northwest, Hammond, U.S.A.

T. Cheng, J. Dolen, N. Parashar

Rice University, Houston, U.S.A.

Z. Chen, K.M. Ecklund, S. Freed, F.J.M. Geurts, M. Kilpatrick, W. Li, B. Michlin, B.P. Padley, J. Roberts, J. Rorie, W. Shi, Z. Tu, J. Zabel, A. Zhang

University of Rochester, Rochester, U.S.A.

A. Bodek, P. de Barbaro, R. Demina, Y.t. Duh, J.L. Dulemba, C. Fallon, T. Ferbel, M. Galanti, A. Garcia-Bellido, J. Han, O. Hindrichs, A. Khukhunaishvili, K.H. Lo, P. Tan, R. Taus, M. Verzetti

Rutgers, The State University of New Jersey, Piscataway, U.S.A.

A. Agapitos, J.P. Chou, Y. Gershtein, T.A. Gómez Espinosa, E. Halkiadakis, M. Heindl, E. Hughes, S. Kaplan, R. Kunnawalkam Elayavalli, S. Kyriacou, A. Lath, R. Montalvo, K. Nash, M. Osherson, H. Saka, S. Salur, S. Schnetzer, D. Sheffield, S. Somalwar, R. Stone, S. Thomas, P. Thomassen, M. Walker

University of Tennessee, Knoxville, U.S.A.

A.G. Delannoy, J. Heideman, G. Riley, K. Rose, S. Spanier, K. Thapa

Texas A&M University, College Station, U.S.A.

O. Bouhali[71], A. Celik, M. Dalchenko, M. De Mattia, A. Delgado, S. Dildick, R. Eusebi, J. Gilmore, T. Huang, T. Kamon[72], S. Luo, R. Mueller, Y. Pakhotin, R. Patel, A. Perloff, L. Perniè, D. Rathjens, A. Safonov, A. Tatarinov

Texas Tech University, Lubbock, U.S.A.

N. Akchurin, J. Damgov, F. De Guio, P.R. Dudero, S. Kunori, K. Lamichhane, S.W. Lee, T. Mengke, S. Muthumuni, T. Peltola, S. Undleeb, I. Volobouev, Z. Wang

Vanderbilt University, Nashville, U.S.A.

S. Greene, A. Gurrola, R. Janjam, W. Johns, C. Maguire, A. Melo, H. Ni, K. Padeken, J.D. Ruiz Alvarez, P. Sheldon, S. Tuo, J. Velkovska, M. Verweij, Q. Xu

JHEP11(2018)042

University of Virginia, Charlottesville, U.S.A.

M.W. Arenton, P. Barria, B. Cox, G. Dezoort, R. Hirosky, H. Jiwon, M. Joyce, A. Ledovskoy, H. Li, C. Neu, T. Sinthuprasith, Y. Wang, E. Wolfe, F. Xia

Wayne State University, Detroit, U.S.A.

R. Harr, P.E. Karchin, N. Poudyal, J. Sturdy, P. Thapa, S. Zaleski

University of Wisconsin — Madison, Madison, WI, U.S.A.

M. Brodski, J. Buchanan, C. Caillol, D. Carlsmith, S. Dasu, L. Dodd, B. Gomber, M. Grothe, M. Herndon, A. Hervé, U. Hussain, P. Klabbers, A. Lanaro, A. Levine, K. Long, R. Loveless, T. Ruggles, A. Savin, N. Smith, W.H. Smith, N. Woods

†: Deceased
1: Also at Vienna University of Technology, Vienna, Austria
2: Also at IRFU, CEA, Université Paris-Saclay, Gif-sur-Yvette, France
3: Also at Universidade Estadual de Campinas, Campinas, Brazil
4: Also at Federal University of Rio Grande do Sul, Porto Alegre, Brazil
5: Also at Université Libre de Bruxelles, Bruxelles, Belgium
6: Also at University of Chinese Academy of Sciences, Beijing, China
7: Also at Institute for Theoretical and Experimental Physics, Moscow, Russia
8: Also at Joint Institute for Nuclear Research, Dubna, Russia
9: Also at Suez University, Suez, Egypt
10: Now at British University in Egypt, Cairo, Egypt
11: Also at Zewail City of Science and Technology, Zewail, Egypt
12: Also at Department of Physics, King Abdulaziz University, Jeddah, Saudi Arabia
13: Also at Université de Haute Alsace, Mulhouse, France
14: Also at Skobeltsyn Institute of Nuclear Physics, Lomonosov Moscow State University, Moscow, Russia
15: Also at CERN, European Organization for Nuclear Research, Geneva, Switzerland
16: Also at RWTH Aachen University, III. Physikalisches Institut A, Aachen, Germany
17: Also at University of Hamburg, Hamburg, Germany
18: Also at Brandenburg University of Technology, Cottbus, Germany
19: Also at MTA-ELTE Lendület CMS Particle and Nuclear Physics Group, Eötvös Loránd University, Budapest, Hungary
20: Also at Institute of Nuclear Research ATOMKI, Debrecen, Hungary
21: Also at Institute of Physics, University of Debrecen, Debrecen, Hungary
22: Also at Indian Institute of Technology Bhubaneswar, Bhubaneswar, India
23: Also at Institute of Physics, Bhubaneswar, India
24: Also at Shoolini University, Solan, India
25: Also at University of Visva-Bharati, Santiniketan, India
26: Also at Isfahan University of Technology, Isfahan, Iran
27: Also at Plasma Physics Research Center, Science and Research Branch, Islamic Azad University, Tehran, Iran
28: Also at Università degli Studi di Siena, Siena, Italy
29: Also at Kyunghee University, Seoul, Korea
30: Also at International Islamic University of Malaysia, Kuala Lumpur, Malaysia
31: Also at Malaysian Nuclear Agency, MOSTI, Kajang, Malaysia
32: Also at Consejo Nacional de Ciencia y Tecnología, Mexico city, Mexico

JHEP11(2018)042

33: Also at Warsaw University of Technology, Institute of Electronic Systems, Warsaw, Poland
34: Also at Institute for Nuclear Research, Moscow, Russia
35: Now at National Research Nuclear University 'Moscow Engineering Physics Institute' (MEPhI), Moscow, Russia
36: Also at St. Petersburg State Polytechnical University, St. Petersburg, Russia
37: Also at University of Florida, Gainesville, U.S.A.
38: Also at P.N. Lebedev Physical Institute, Moscow, Russia
39: Also at California Institute of Technology, Pasadena, U.S.A.
40: Also at Budker Institute of Nuclear Physics, Novosibirsk, Russia
41: Also at Faculty of Physics, University of Belgrade, Belgrade, Serbia
42: Also at INFN Sezione di Pavia [a], Università di Pavia [b], Pavia, Italy
43: Also at University of Belgrade, Faculty of Physics and Vinca Institute of Nuclear Sciences, Belgrade, Serbia
44: Also at Scuola Normale e Sezione dell'INFN, Pisa, Italy
45: Also at National and Kapodistrian University of Athens, Athens, Greece
46: Also at Riga Technical University, Riga, Latvia
47: Also at Universität Zürich, Zurich, Switzerland
48: Also at Stefan Meyer Institute for Subatomic Physics (SMI), Vienna, Austria
49: Also at Adiyaman University, Adiyaman, Turkey
50: Also at Istanbul Aydin University, Istanbul, Turkey
51: Also at Mersin University, Mersin, Turkey
52: Also at Piri Reis University, Istanbul, Turkey
53: Also at Gaziosmanpasa University, Tokat, Turkey
54: Also at Ozyegin University, Istanbul, Turkey
55: Also at Izmir Institute of Technology, Izmir, Turkey
56: Also at Marmara University, Istanbul, Turkey
57: Also at Kafkas University, Kars, Turkey
58: Also at Istanbul Bilgi University, Istanbul, Turkey
59: Also at Hacettepe University, Ankara, Turkey
60: Also at Rutherford Appleton Laboratory, Didcot, United Kingdom
61: Also at School of Physics and Astronomy, University of Southampton, Southampton, United Kingdom
62: Also at Monash University, Faculty of Science, Clayton, Australia
63: Also at Bethel University, St. Paul, U.S.A.
64: Also at Karamanoğlu Mehmetbey University, Karaman, Turkey
65: Also at Utah Valley University, Orem, U.S.A.
66: Also at Purdue University, West Lafayette, U.S.A.
67: Also at Beykent University, Istanbul, Turkey
68: Also at Bingol University, Bingol, Turkey
69: Also at Sinop University, Sinop, Turkey
70: Also at Mimar Sinan University, Istanbul, Istanbul, Turkey
71: Also at Texas A&M University at Qatar, Doha, Qatar
72: Also at Kyungpook National University, Daegu, Korea

JHEP11(2018)042